ALMA MATER STUDIORUM - UNIVERSITÀ DI BOLOGNA

SCUOLA DI INGEGNERIA E ARCHITETTURA

Sede di Forlì

CORSO DI LAUREA IN INGEGNERIA AEROSPAZIALE
CLASSE L-9

ELABORATO FINALE DI LAUREA

In

TERMOFLUIDODINAMICA AVANZATA E CONTROLLI TERMICI LM

Design and fluid dynamic analysis of a custom drip chamber in a medical disposable device

CANDIDATO

Gabriele Guerra

RELATORE

Prof. Marco Lorenzini

CORRELATORI

Prof. Marco Troncossi
Ing. Jose Vicente Farina

Anno Accademico 2014/15

Sessione II^{a}

Per quanto il vento ululi forte,
una montagna non può inchinarsi ad esso.

Sommario

Negli ultimi anni, parallelamente allo sviluppo di calcolatori elettronici sempre più performanti, la fluidodinamica computazionale è diventata uno strumento di notevole utilità nell'analisi dei flussi. Si è inoltre dimostrata di importante ausilio nello sviluppo di dispositivi medici. Quando impiegate nello studio di flussi di fluidi fisiologici, come quello del sangue, il vantaggio principale delle analisi CFD è che permettono di caratterizzare il comportamento fluidodinamico senza dover eseguire test in-vivo/in-vitro, consentendo quindi notevoli vantaggi in termini di tempo, denaro e rischio derivante da applicazioni mediche. Inoltre, simulazioni CFD offrono una precisa e dettagliata descrizione di ogni parametro di interesse permettendo, già in fase di progettazione, di prevedere quali modifiche al layout garantiranno maggiori vantaggi in termini di funzionalità. Il presente lavoro di tesi si è posto l'obiettivo di valutare, tramite simulazioni CFD, le performances fluidodinamiche del comparto sangue "camera venosa" di un dispositivo medico monouso Bellco impiegato nella realizzazione di trattamenti di emodialisi. Al fine di offrire al lettore una panoramica del contesto, il primo capitolo dell'elaborato presenta una breve descrizione della disfunzione renale e dei trattamenti sostitutivi. Notevole impegno è stato in seguito rivolto allo studio della letteratura scientifica in modo da definire un modello reologico per il fluido non-Newtoniano preso in considerazione e determinarne i parametri caratteristici. Il terzo capitolo presenta lo stato dell'arte delle apparecchiature Bellco, rivolgendosi con particolare attenzione al componente "cassette" del dispositivo monouso. L'analisi fluidodinamica del compartimento "camera venosa" della cassette, che sarà presa in considerazione nei capitoli quinto e sesto, si inserisce nell'ambito della riprogettazione del dispositivo attualmente in commercio: il quarto capitolo si incentra sul suo nuovo design, ponendo specifico interesse sul layout della camera venosa di nuova generazione. Per lo studio dei flussi che si sviluppano internamente ad essa ci si è avvalsi del modulo CFD del software COMSOL multiphysics® (versione 5.0); la definizione del modello implementato e della tipologia di studio effettuato sono presi in considerazione nel quinto capitolo. Le proble-

matiche di maggior impatto nella realizzazione di un trattamento di emodialisi sono l'emolisi e la coagulazione del sangue. Nell'evenienza che si verifichino massivamente occorre infatti interrompere il trattamento con notevoli disagi per il paziente, per questo devono essere evitate. Nel sesto capitolo i risultati ottenuti sono stati esaminati rivolgendo particolare attenzione alla verifica dell'assenza di fenomeni che possano portare alle problematiche suddette.

Abstract

In recent years, together with the development of more efficient computer, Computational Fluid Dynamics (CFD) has become a considerably useful tool in the analysis of flows. It has also proved to be of much help in the development of medical devices. When used in the study of physiological fluids flows, such as blood, the main advantage of CFD analysis is that they allow the characterization of the fluid-dynamic behavior without the need of in-vivo/in-vitro measurements, leading to considerable benefits in terms of time, money and risk arising from medical applications. In addition, CFD simulations offer an accurate and detailed description of each parameter of interest. Starting from the design phase, it is possible to predict what layout changes will lead to greater advantages in terms of functionality. The present work has the purpose of assessing, by means of CFD simulations, the fluid- dynamic performances of the blood compartment "venous chamber" of a Bellco's medical disposable device used in carrying out hemodialysis treatments. In The first chapter, a brief description of kidney failure and its replacement therapy provides the reader an overview of the context in which this thesis work has been developed. Considerable effort was then addressed to the study of the scientific literature, so as to define a rheological model for the non-Newtonian fluid taken into consideration and to determine its characteristic parameters. The third chapter deals with the Bellco's equipment state of the art, focusing on the disposable device component "cassette". The fluid dynamic analysis of the venous chamber of the cassette is part of the redesign of the currently used device: the fourth chapter focuses on its new layout, particularly that of the new venous chamber. The investigations on the flows that develop inside the venous chamber were done using the CFD module of the software COMSOL Multiphysics® (version 5.0); the definition of the implemented model and the type of study are taken into account in the fifth chapter. The major problems during an extracorporeal dialysis treatment are blood hemolysis and coagulation. If they occur massively, it is necessary to suspend the treatment, with considerable troubles for the patient; therefore, they must be avoided. In

the sixth chapter, the obtained results are examined focusing on checking the absence of phenomena that can lead to the above-mentioned problems.

Contents

List of abbreviations

AKI Acute kidney injury

ARF Acute renal failure

μ_{app} Apparent Viscosity

BHD Bicarbonate Hemodialysis

K_c Casson viscosity coefficient

CKD Chronic kidney disease

CFD Computational Fluid Dynamics

μ Dynamic Viscosity

ESRD End-stage renal disease

$l_{e,lam}$ Entrance length for Laminar flow

FEM Finite Element Method

ρ Fluid Density

GFR Glomerular filtration rate

H Hematocrit

HD Hemodialysis

HF Hemofiltration

HDF Hemodiafiltration

μ_∞ Infinite-shear-rate viscosity

ν Kinematic Viscosity

$\dot{m}$ Mass Flow Rate

PDEs Partial Differential Equations

RBC Red blood cell

Re Reynolds Number

$\dot{\gamma}$ Shear Strain

τ Shear Stress

τ_t Threshold Shear Stress for Erythrocytes damage

τ_0 Yield Stress

WBC White blood cell

μ_0 Zero-shear-rate viscosity

List of Figures

List of Tables

Preface

This thesis work was done in collaboration with the R&D Disposable Department at the company Bellco, Mirandola. Bellco is an Italian company with more than 40 years experience which has been a pioneer in the history of dialysis. Nowadays, Bellco operates worldwide as a leader in the field of advanced therapies, playing a key role in supplying hemodialysis and intensive care products. My collaboration with the Bellco R&D Department has started and developed thanks to Eng. Jose Vicente Farina, to whom i express my gratitude. I would like to thank him for his friendship, for his support and for the time he dedicated to me, answering patiently to all the questions I posed. I am also very grateful to Professors Marco Lorenzini and Marco Troncossi for being my supervisors, for giving me the opportunity to develop this thesis and for all the help they gave me.

Chapter 1

Kidney Failure and Dialysis

This chapter introduces reader to renal failure and its replacement therapy: dialysis.

Kidneys are two organs with the average size of a fist located in the abdominal cavity (see Fig.1.1). Blood is transported to the kidneys through the renal (arcuate) artery an returns to the heart through the renal (arcuate) vein and the lower vena cava. Their main function is to remove excess water and waste products of metabolism, such creatinine and urea, from blood. Besides, they also maintain the homoeostasis of electrolytes removing several salts and regulate the acid-base balance. In addition, human kidneys perform a few endocrine and metabolic functions, such as production of the hormone known as erythropoietin and conversion of vitamin D to its active form [33]. Each kidney contains about 1 million nephrons (see Fig.1.2), each nephron being capable of forming urine by itself. The nephron is composed of a glomerulus (a capillary bed) through which fluid is filtered out of the blood and a long tubule in which the filtered fluid is converted into urine on its way to the pelvis of the kidney; from here two small tubes called ureters carry the waste matter to the bladder, which expels the urine through the urethra. [55].

1.1 Kidney Failure

Kidney failure is a medical condition in which the kidneys fail to perform their task adequately. This is mainly determined by a decrease

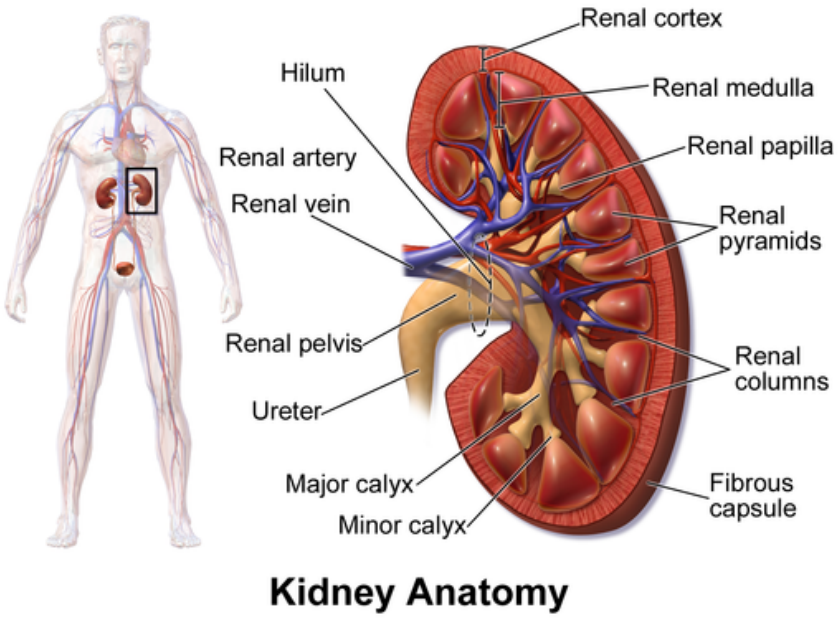

Figure 1.1: Representative image of a Kidney [8].

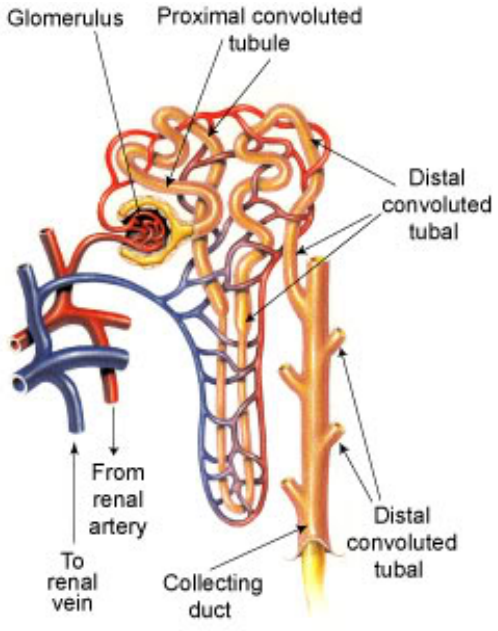

Figure 1.2: The Nephron and its components [62].

in glomerular filtration rate (GFR) that is the rate at which blood is filtered in the glomeruli of the kidneys; symptoms are a decrease in or absence of urine production and determination of waste products (creatinine or urea) in the blood. There may be also problem with increased fluid in the body leading to swelling, raised levels of potassium, decreased levels of calcium and in later stages anaemia. Long-term kidney problems are also associated with increased risk of cardiovascular disease [31].

Renal failure can be divided into two categories: acute kidney injury, which is often reversible with adequate treatment, and chronic kidney disease, which is often not reversible.

1.1.1 Acute Kidney Injury

Acute kidney injury (AKI) or acute renal failure (ARF) [6] is a rapidly progressive loss of renal function generally characterized by a decrease in urine production and fluid electrolyte imbalance [44]. AKI usually occurs when the blood supply to the kidneys is suddenly interrupted (for example accidents, injuries or complications from surgeries in which the kidneys are deprived of normal blood flow for extended periods of time) or when the kidneys become overloaded with toxins (drug overdose, chemotherapy). People suffering from acute kidney injury require supportive treatment until their kidneys recover function, and they often remain at increased risk of developing future kidney failure [57].

1.1.2 Chronic Kidney Disease

Chronic kidney disease (CKD) is a progressive loss in renal function over a period of months or years. The most common causes of CKD are diabetes and long-term, uncontrolled hypertension [4]; overuse of common drugs such as ibuprofen and paracetamol can also cause chronic kidney disease [34]. Some infectious disease, such as Hantavirus and HIV, can attack the kidneys, causing renal failure. Chronic kidney disease is identified by a blood test for creatinine, which is a breakdown product of muscle metabolism. Higher levels of creatinine indicate a

lower GFR and as a result a decreased capability of the kidneys to excrete waste products. As summed-up in Tab.1.1, the severity of CKD is measured in five stages, which are calculated using patient's GFR [16].

Stage 1 CKD is mildly diminished renal function with few symptoms; Stages 2 and 3 need increasing levels of supportive care from their medical providers to slow and treat their renal dysfunction. Patients in stages 4 and 5 usually require preparation of the patient towards active treatment in order to survive. Stage 5 CKD, often-called *end-stage renal disease* (ESRD), is considered a severe illness with poor life expectancy if untreated and requires some form of renal replacement therapy (dialysis) or kidney transplant whenever feasible.

Chronic kidney disease resulted in 956'000 deaths in 2013 up from 409'000 deaths in 1990 [17]. In 2012, patients reported under ESRD were approximately 42'000 in Italy [63]; in Canada 1.9 to 2.3 million people have CKD [2]. The U.S. Centers for Disease Control and prevention found that CKD affected an estimated 16.87% of U.S. adults aged 20 years and older, during 1999 to 2004 [18].

1.2 Treatment for End-Stage Renal Disease

There are several treatments for end-stage renal disease which allow extending the life of the patients for some years, kidney transplantation being the best alternative [52]. However, this option is limited by the number of kidneys available and by the compatibility with the donor. This way, dialysis treatments have to be done, where the function of kidneys is mimicked artificially.

Table 1.1: GFR level for different CKD stage

CKD Stage	***GFR level*(mL/min/1.73 m^2)**
Stage 1	$\geq$90
Stage 2	60 – 89
Stage 3	30 – 59
Stage 4	15 – 29
Stage 5	$<$15

Dialysis is a process for removing waste and excess fluid from the blood and is used primarily as an artificial replacement for lost kidney function in people with kidney failure. The underlying principles of dialysis is the diffusion of solutes and ultra-filtration of fluid across a semi-permeable membrane. Diffusion is a property of substance in water: they tend to move from an area of high concentration to an area of low concentration. Blood flows by one side of a semi-permeable membrane, and dialysate[1], or special dialysis fluid, flows by the opposite side. A semi-permeable membrane is a thin layer of material that contains holes of various sizes, or pores. Smaller solutes and fluid pass through the membrane, but the membrane blocks the passage of larger substances (for example, red blood cells, large proteins). This replicates the filtering process that takes place in the kidneys, when the blood enters the kidneys and the larger substances are separated from the smaller ones in the glomerulus [41].

There exist different kinds of dialysis: peritoneal dialysis, hemodialysis, hemofiltration and hemodiafiltration.

1.2.1 Peritoneal Dialysis

In peritoneal dialysis, the dialysate runs through a tube into the peritoneal cavity[2] where the peritoneum acts as a partially permeable membrane. Diffusion and osmosis drive waste products and excess fluid through the peritoneum into the dialysate until it approaches equilibrium with the body's fluids. Then the dialysate is drained, discarded, and replaced with fresh dialysate [32]. A schematic view of a peritoneal dialysis treatment is summed in Fig. 1.3.

1.2.2 Hemodialysis (HD)

In hemodialysis blood is pumped out of the body to an external filter, called dialyzer, where it flows in the lumen of thousands of tiny hol-

[1] *Dialysate*: a chemical bath used in dialysis to draw fluids and toxins out of the bloodstream and supply electrolytes and other chemicals to the bloodstream [25].

[2] *Peritoneal cavity*: a potential space between the parietal peritoneum and visceral peritoneum [54], that is, the two layer of tissue containing blood vessels that lines and surrounds the abdominal cavity and the relatives internal organs (stomach, spleen, liver, intestine) [7].

low fibres membranes (0.4 – 2.6 m^2 surface area) while the dialysate counter-flows in the dialyzer's shell. The hollow fibre membrane acts as a barrier that retains blood proteins and cells, while removing low molecular weight waste metabolites from the blood to the dialysate [1]. The counter-current flow of the blood and the dialysate maximizes the concentration gradient of solutes between the blood and dialysate, which help remove more toxins from the blood. The concentrations of solutes are high in the blood, but low or absent in the dialysis solution and constant replacement of the dialysate ensure that the concentration of undesired solutes is kept low on this side of the membrane. In order to prevent the depletion of the blood electrolytes, the dialysate should contain a similar concentration of minerals like potassium and calcium. This treatment is very effective removing small uremic toxins, but for larger toxins the removal is low, due to the sieving properties of the membrane. For the filtration of excess water, a transmembrane pressure difference can be applied, controlling easily the amount of water removed [13]. After filtration, the cleansed blood is returned via the circuit back to the patient's body (see Fig.1.4).

Hemodialysis is the most common treatment for end stage renal disease, with nearly 1,4 million uretic patients treated worldwide in 2004 [13].

1.2.3 Hemofiltration (HF)

Hemofiltration is a similar treatment to hemodialysis, but it works according to a different principle. The blood is pumped through a dialyzer as in hemodialysis but no dialysate is used. A pressure gradient - called transmembrane pressure - is applied and, as a result, water and solute move across the ultrafiltration membrane by a convective mechanism (see Fig.1.5). Hemofiltration membranes are usually 10 times more permeable to plasma water than the membrane for hemodialysis; however, they should be capable of retaining the blood proteins and cells [13] as well.

Since the main mechanism of removal is convection, dissolved substances with large molecular weight, which are not cleared as well in hemodialysis, are filtered. On the other hand, small molecules are just

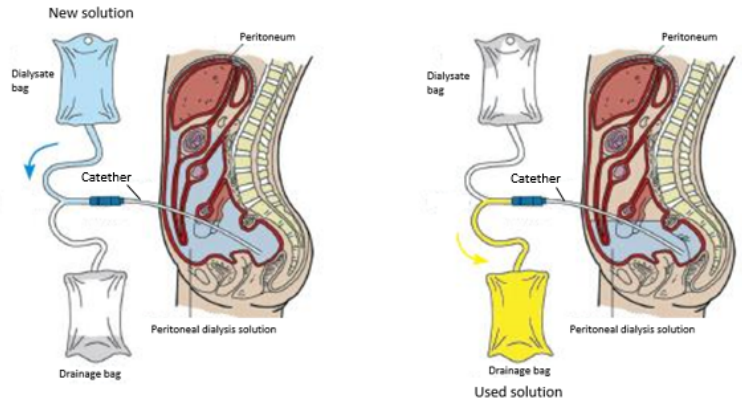

Figure 1.3: Schematic of a peritoneal dialysis treatment [64].

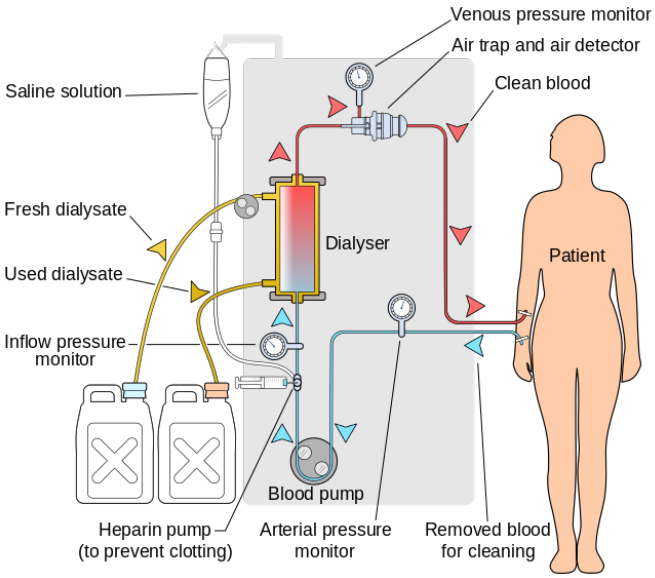

Figure 1.4: Schematic of a hemodialysis treatment [61]

dragged from the water flux, the concentration in the filtrate being similar to tat of the plasma. This implies that the removal of small molecules is not as efficient as in the hemodialysis [13].

Due to higher plasma water loss, the ultrafiltrate produced has to be completely or partially replaced by a replacement fluid containing electrolytes. The replacement fluid can be introduced in the blood upstream (pre-dilution), downstream (post-dilution) or in both at the same time [13] [28].

1.2.4 Hemodiafiltration (HDF)

Hemodiafiltration is a combination of the treatments hemodialysis and hemofiltration [23]. To improve the poor removal of low molecular weight solutes in hemofiltration, a dialysate fluid is circulated in the counter-flow shell of a hemofilter originating a concentration gradient that causes the diffusion of small molecular weight solutes out of the blood [33]. On the other hand, the convective flow imposed in this method results in a better deduction of the excess water and the higher molecular weight toxins [23].

As in hemofiltration, a replacement fluid may be needed. This substitution fluid can also be administered either before, after or both before and after the dialyzer. Both pre-dilution and post-dilution have advantages and disadvantages: pre-dilution has the advantage of decreasing blood viscosity and hemoconcentration preventing clot formation in the membrane but has the disadvantage of diluting the blood toxins, reducing their clearances [19]. On the other hand, during post-dilution the higher hemoconcentration and viscosity enhance diffusive flux (there is a higher concentration gradient between blood and dialysate) but limit the convective flux achieving larger clearances for low molecular weight and lowest clearances for medium molecular weight toxins [21] [48].

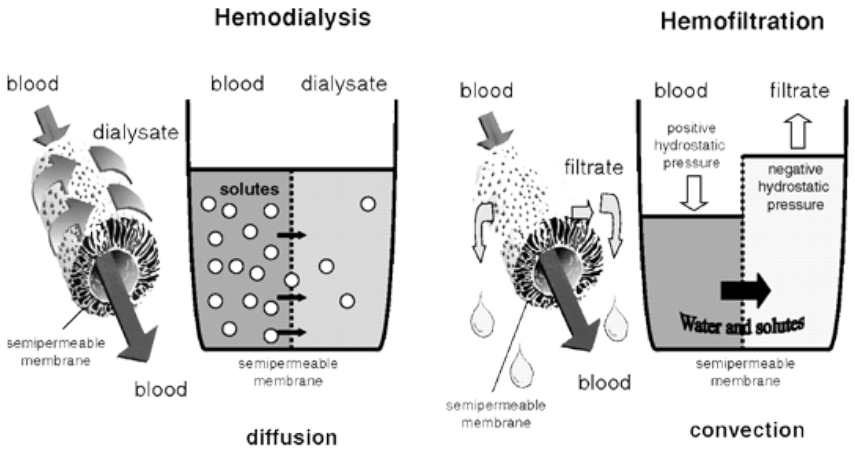

Figure 1.5: Difference between hemodialysis and hemofiltration [59]

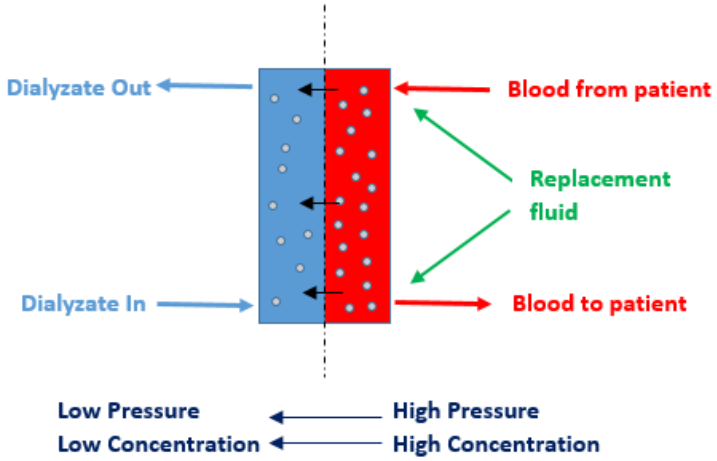

Figure 1.6: Working principle of hemodiafiltration [65]

Chapter 2

Blood Rheology

In the previous chapter, kidney disease and its replacement therapy were examined. It has been pointed out that in healthy people renal function carries out toxins removal from blood circulating inside kidneys while in those with renal dysfunction, blood is cleaned through a hemofilter. It is therefore necessary to detail the physical properties of blood that define its fluid dynamics performance characteristics. The aim of this chapter is to introduce the vast field of blood rheology[1], and define the model and the relative parameters that shall be used in the simulation. Moreover, the final sections deal with the relations between fluid-dynamic characteristics and problems associated with blood extra-corporeal circulation, such as hemolysis and coagulation. To this aim, this chapter deals with:

- *Blood compostion*: whole blood consists of a suspension of 40-50% by volume of small deformable bodies, mainly red cells in the transparent plasma [55]. The rheological characteristics of blood are determined by the properties of this components and their interaction with each other as well as with the surrounding structures [51];

- *Physiological fluid dynamics and Hemorheology*: while plasma is

[1] *Rheology* is the study of the flow of matter, primarily in a liquid state, but also as 'soft solids' or solids under conditions in which they respond with plastic flow rather than deforming elastically in response to an applied force [49]. In particular *Hemorheology* deals with the flow and deformation behaviour of blood and its formed elements (RBCs, WBCs, platelets).

generally treated as a Newtonian fluid, the behaviour of whole blood is *non-Newtonian* hence is needed to define its non-Newtonian rheological characteristics;

- *Hemolisys*: hemolysis refers to the breakdown of red blood cells and the consequent release of hemoglobin in plasma. Conditions that can cause hemolysis include immune reactions, toxins and mechanical stresses (such as those deriving from hemodialysis);

- *Coagulation*: coagulation relates to the process by which a blood clot is formed. It results from a complex cascade reaction, that involves many 'clotting factors', some always present in the blood and some released from damaged tissue and platelets.

2.1 Blood composition

In order to acquire better understanding of the non-Newtonian behavior of blood it is necessary to specify its components. Blood is about 7% of the human body weight. The normal adult has a blood volume of about 5 litres [37]. Blood is a circulating heterogeneous multi-phase mixture of formed elements (corpuscles or cells) suspended in a fluid medium known as plasma (about 55% by volume; 2.7 - 3.0 litres in a normal human). The formed elements (cells) consist of red blood cells 'RBCs' (erythrocytes), white blood cells 'WBCs' (leukocytes) and platelets (thrombocytes).The formed elements in blood consist of 95% red blood cells, 0.13% white blood cells and about 4.9% platelets.

Plasma is a transparent, slightly yellowish, dilute electrolyte solution (almost 92% water) containing organic molecules, minerals and the three major types of blood proteins: fibrinogen, globulin and albumin [51] [55].

RBCs are produced in the bone marrow and consist of a concentrated solution of haemoglobin, an oxygen carrying protein, surrounded by a flexible membrane. Their typical dimensions in humans are $7.8\mu m$ in diameter and $2\mu m$ in thickness [55]. Their shape is that of biconcave discoid, flexible enough to vary depending on the diameter of the vessel through which blood is flowing. RBCs are the dominant partic-

ulate matter in blood, numbering approximately $5 \cdot 10^6$ per mm^3. The percentage of blood volume made up by red cells is referred to as the hematocrit. Hematocrit ranges from 42 to 45% in normal blood, and plays a major role in determining the rheological properties of blood [37].

WBCs are cells of the immune system which defend body against both infectious disease and foreign materials. Several different type of leukocytes exist and they are all produced in the bone marrow. Their size vary from 6 to 22 μm. There are normally 10^4 white blood cells per mm^3 of blood, so that their volume concentration in the blood is one white cell to every 1000 red cells, which is totally insignificant from the rheological point of view [37] [55].

Platelets are cells fragments circulating in blood that are involved in the cellular mechanism of haemostasis leading to the formation of clots. Low levels of platelets predisposes to bleeding, while high levels increase the risk of thrombosis (that is the coagulation of blood in the heart or blood vessel). They are much smaller than red or white cells, whit a diameter of 2-3 μm. Their number is one-tenth of the red cells [37].

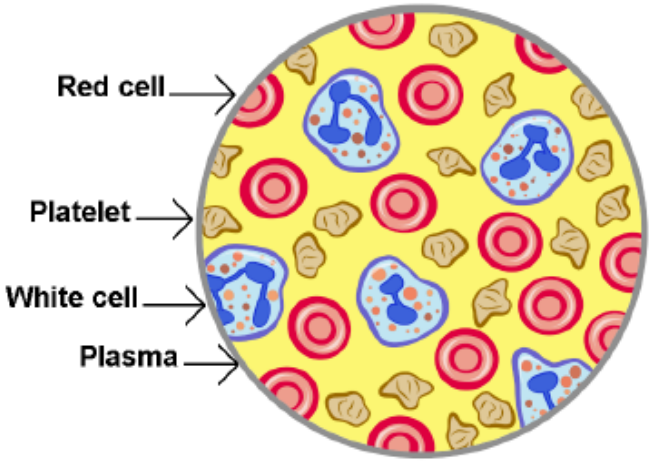

Figure 2.1: Simplified illustration of the main blood composition [51].

2.2 Physiological fluid dynamics and Hemorheology

Physiological fluid dynamics deals with flow of biological fluids, for example, blood in a tube such as blood vessel. The involved physical quantities like velocity profiles, flow rates and pressures depend on the nature of fluid and the existing internal forces; it is therefore essential to understand the rheological properties of the fluid in the presence of forces. The basic difference between the solid and the fluid state is that the former may exert a restraining force on the displaced plane inside the medium, while the latter is unable to sustain internal forces. The concept of solidity and fluidity are idealizations that describe the behaviour of real materials in certain limiting cases. Figure 2.2 summarizes the types of rheological materials. In general, the be-

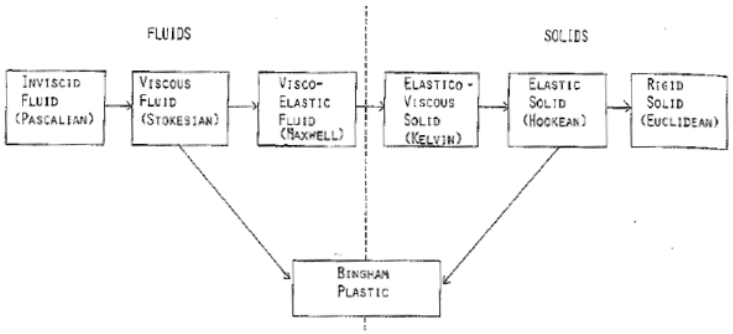

Figure 2.2: Rheological classification of materials [55].

haviour of real materials encompasses many intermediate properties of those shown in the figure. A rigid solid does not deform under shear or tangential force. An elastic medium deforms under stress but returns to its original state when the stress is removed. An inviscid fluid has zero viscosity which represent another extreme of a material. Bingham plastic remains rigid when the shear stress is of smaller magnitude then the yield value τ_0 but flows like a Newtonian fluid when the shear stress exceeds τ_0 [55].

Blood's rheological properties do not allow a clear classification according to the scheme in figure 2.2: in fact many different methods exist to describe its behaviour. In the next sections differences between New-

tonian and non-Newtonian fluids are elucidated, then non-Newtonian characteristics of blood are investigated and a constitutive equation is chosen in order to describe blood flow behaviour.

2.2.1 Newtonian and non-Newtonian fluids

According with the categorization illustrated in figure 2.2, an inviscid fluid is one that has no viscosity. With zero viscosity, the fluid offers no resistance to shearing forces. Hence, all shear forces are zero during flow and deformation of the fluid. However, all real fluids have finite viscosity, and it is necessary to take into account the viscosity and the related shear forces associated with its deformation. Real fluids are also called viscous fluids. Considering only laminar flow conditions, a shear stress - shear rate relationship is used to define the fluidity of liquids. This relation reflects the internal resistance between fluid layers (laminas) and thus reflects the viscosity of the fluid; the viscosity of a liquid can be calculated by dividing the shear stress by the shear rate.

From a rheological point of view, real fluids are classified into two main categories. *Newtonian fluids* are characterized by the *shear stress* τ, which is proportional to the *shear strain* $\dot{\gamma}$ (also called shear rate). The slope of the characteristic represents the viscosity coefficient μ which is constant at a given temperature and pressure. τ refers to the shear forces per unit area, while the rate of shear strain $\dot{\gamma}$ signifies the velocity decrease in the distance perpendicular to the direction of flow. The shear stress - shear rate relationship can be described by the equation

$$\tau = -\mu\dot{\gamma} \tag{2.1}$$

This is known as Newton's law of viscosity, and fluids that behave in this fashion are termed Newtonian fluids. There are, however, many fluids whose rheological behaviour does not obey equation (2.1) and the are referred to as non-Newtonian fluids. As stated in the introduction of this chapter, while plasma acts like a Newtonian fluid, whole blood is treated as non-Newtonian. *Non-Newtonian fluids* are those in which the viscosity is not a constant but rather depends on the magnitude of

either τ or $\dot{\gamma}$. The slope of the shear stress - shear rate characteristic calculated at any given point on the curve is called *apparent viscosity*, μ_{app} at that point, which reads

$$\mu_{app} = \tau/\dot{\gamma}$$

The apparent viscosity of a non-Newtonian fluid may decrease (*shear thinning* behaviour) or increase (*shear thickening* behaviour) as the shear rate is increased. Non-Newtonian fluids may also have a yield stress below which there is a finite stress but the shear rate is zero (no flow), resulting in an infinite value for apparent viscosity. Note that for both classes of fluids, the viscosity depends on temperature and for most fluids viscosity decrease with increasing temperature. All these information are displayed in figure 2.3 and 2.4.

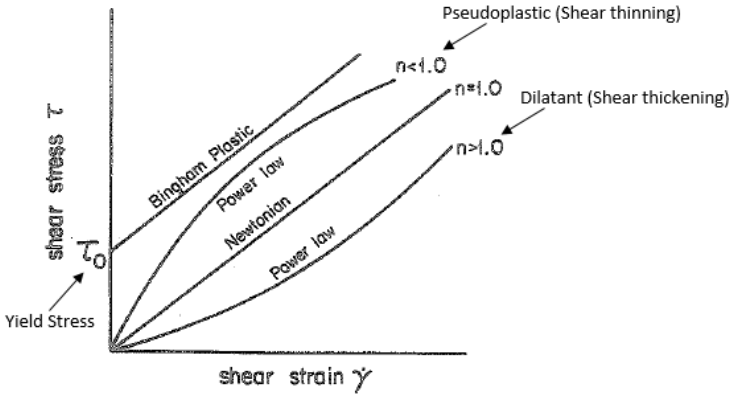

Figure 2.3: Shear stress / Shear Strain relationship for Newtonian and non-Newtonian fluids [55].

2.2.2 Modeling blood

The apparent viscosity of blood depends on the viscosity of the plasma, the hematocrit (Fig. 2.5), the shear rate (Fig.2.5), the narrowness of the vessel in which it is flowing (the so called Fahraeus-Lindqvist effect, Fig.2.6) and on the temperature. The dependence on the prevailing shear rate and the Fahraeus-Lindqvist effect classify blood as a non-Newtonian fluid. As mentioned in Section 2.1, most non-Newtonian

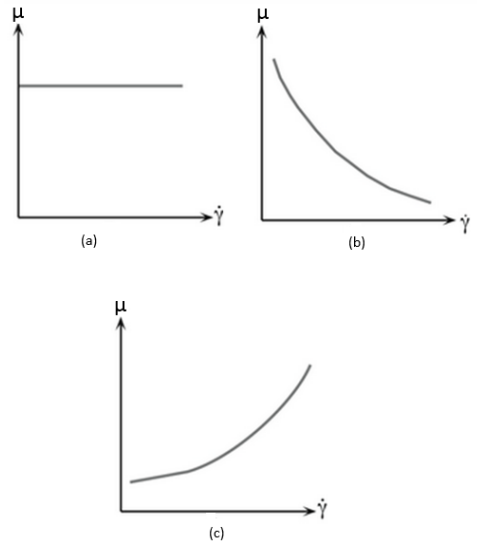

Figure 2.4: Viscosity - Shear Rate relation for (a)Newtonian fluid; (b) Shear thinning fluid; (c) Shear thickening fluid; [60].

effects originate from the RBCs due to their high concentration and distinguished mechanical properties such as elasticity and ability to aggregate forming three-dimensional structures at low deformation rates, while the presence of white blood cells and platelets do not significantly affect the viscosity of blood since they are present in such small proportions. However, platelets play an important role in the formation of blood clots which may severely interfere with the flow [37].

Human blood is a shear thinning fluid. At low shear rates the apparent viscosity is high, whereas under high shear forces viscosity approaches an asymptotic value that correspond to blood viscosity when considered as Newtonian fluid. This shear thinning rheology arises from disaggregation of the red blood cells with increasing shear rate, indeed the aggregation is mostly demonstrated at low shear rates and hence non-Newtonian behaviour is more pronounced at these regimes of low deformation. The relationship between shear stress - shear rates for a sample of human blood is shown in figure 2.7. As can be noticed, the non-Newtonian region is below $100 sec^{-1}$ of shear strain rate; at higher $\dot{\gamma}$ the viscosity of blood is relatively insensitive to further increase of shear. For that reason there seems to be a general consensus that for $\dot{\gamma} > 100\, s^{-1}$ blood can be considered as Newtonian [5], [24], [39], [40],

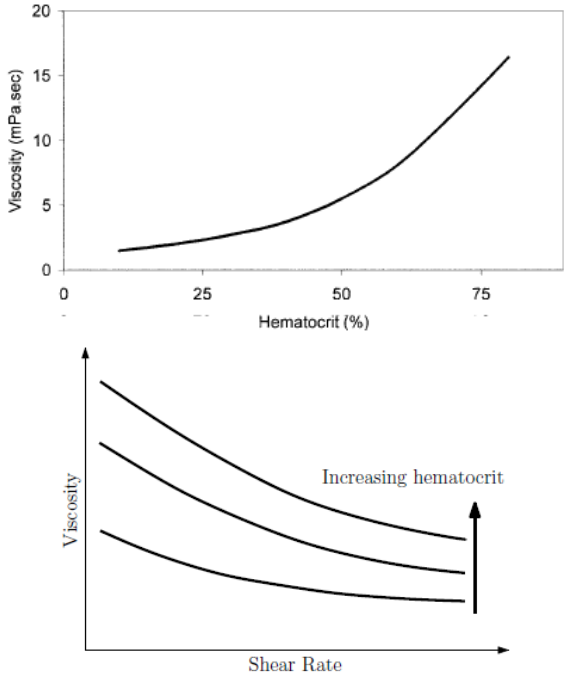

Figure 2.5: (a)Effect of hematocrit on blood viscosity; (b)Human blood viscosity as a function of shear rate for a range of hematocrit concentrations; [5],[51]

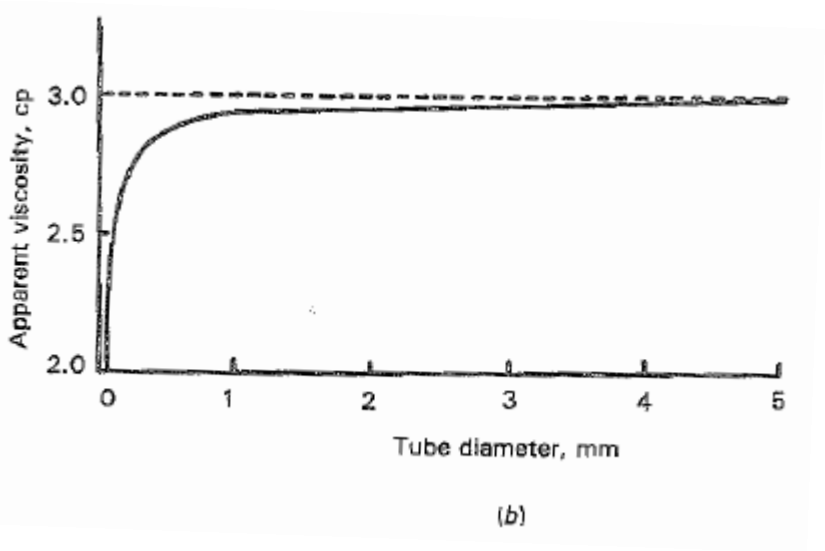

Figure 2.6: Effect of tube diameter on apparent viscosity of blood for $H = 40\%$ $T = 38°C$ [55]. ($1cp = 10^{-3} Pa \cdot s$)

[46], [51]. Many empirical equations and models have been proposed in the last few decades to express this relation between τ and $\dot{\gamma}$, however there is none universally accepted. The most commonly used are the *Casson* model [3], [37], [51], and the *Carreau-Yasuda* model [3], [24], [27], [45], [51], which are briefly explained in the following paragraphs.

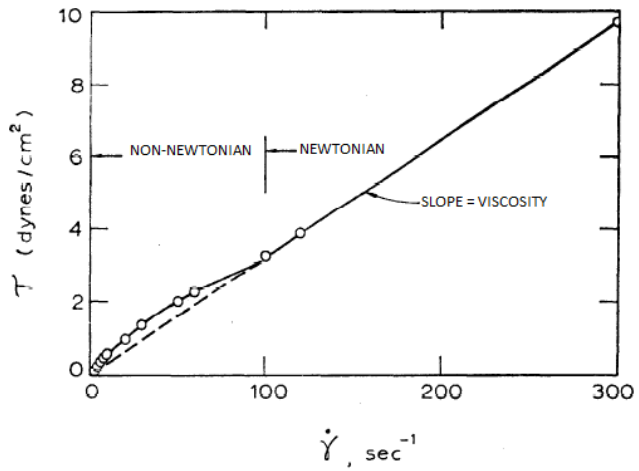

Figure 2.7: τ plotted vs. $\dot{\gamma}$ for $H = 40\%$, $T = 37°C$. Note confusion of points near origin [40]. ($1 dynes/cm^2 = 0.1 Pa \cdot s$)

Casson rheology model is a modified Bingham plastic model in which blood is considered rigid when the shear stress is of smaller magnitude than a yield stress τ_0 but flows like a Newtonian fluid when $\tau > \tau_0$. It is normally used when the non-Newtonian feature to highlight is the presence of the yield stress. The general expression is

$$\sqrt{\tau} = K_c\sqrt{\dot{\gamma}} + \sqrt{\tau_0} \tag{2.2}$$

where

K_c is the Casson viscosity coefficient (a non-dimensional quantity);

τ_0 is the yield stress, function of the hematocrit.

According to the definition of Bingham plastic, $\dot{\gamma}$ is zero if $\tau < \tau_0$. Figure 2.8 represent the so called 'Casson plot', a double square root plot of shear stress vs. shear rate.

The *Carreau-Yasuda* model is used to emphasise the shear thin-

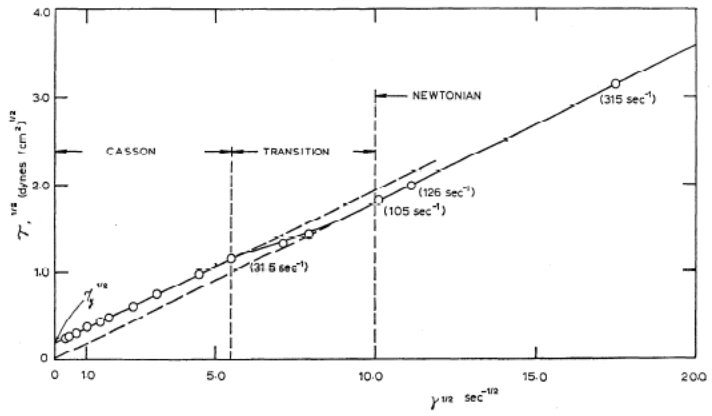

Figure 2.8: Square root of shear stress plotted versus square root of shear rate ($H = 40\%$; $T = 37°C$). Note the determination of square root of yield stress τ_0 by linear extrapolation [40].($1 dynes/cm^2 = 0.1 Pa \cdot s$)

ning feature of blood flow. It suggests the following equation which incorporates two limiting viscosity:

$$\mu(\dot{\gamma}) = \mu_\infty + (\mu_0 - \mu_\infty)[1 + (\lambda\dot{\gamma})^a]^{(\frac{n-1}{a})} \tag{2.3}$$

where

μ_0 is the zero-shear-rate viscosity;

μ_∞ is the infinite-shear-rate viscosity;

λ, a and $n < 1$ (shear thinning index) are curve fitting parameters that define the transition region. The parameters a and n are non-dimensional, the parameter λ has dimensions of time.

The main advantage of the Carreau-Yasuda model over other non-Newtonian blood models is that it is continuous for all $\dot{\gamma} \geq 0$. We note that

$$\lim_{\dot{\gamma}\to 0} \mu(\dot{\gamma}) = \mu_0 \qquad \lim_{\dot{\gamma}\to \infty} \mu(\dot{\gamma}) = \mu_\infty \tag{2.4}$$

indicating that at high shear rates the fluid acts as Newtonian with viscosity μ_∞, whereas at low shear rates, the fluid acts as non-Newtonian with viscosity μ_0. This model is normally used in numerical modelling schemes thanks to its easier implementation due to its continuity [9].

In this work, it is needed to emphasize the shear thinning property of blood, so the Carreau-Yasuda model is chosen. The chosen values for

the parameters that define Equation 2.3 will be presented in chapter 5.

2.3 Haemolisys

Hemolysis refers to the loss, that is, damage of red blood cells [55]. Hemolysis has been thought to be of many origins, including the effect of solid surface interaction, shear stress and high negative pressure gradients [38]. In normal human circulation system, the motion and resulting forces acting on blood components do not destroy them (typical values of the wall shear stress in the normal circulation are found in the range 1-3 Pa), but may even facilitate their function. However, in some diseased state or when circulating in a foreign body (like a hemodialysis circuit), the destruction of blood components occurs and their orderly recycling process is altered. The occurrence of hemolysis is evidenced by elevated serum hemoglobin and the appearance of fragmented cells in the circulating blood called 'ghost cells'.

Many studies have been made on hemolysis, hypotheses have been proposed to explain the mechanism and threshold values for both the shear stress (τ_t) and negative pressure gradient (ΔP) for extensive erythrocytes damage have been identified. Referring to the shear stress, three classes of hemolysis have been identified:

- *Wall-red blood cells interaction*(τ_t <150 Pa): cells that are in physical contact with surfaces are mechanically torn or collapse upon themselves so that modification on their morphology are produced. In this regime of relatively low stresses there is little damage, dependent on the surface condition and contact duration.

- *Prolonged intermediate shear stress* (τ_t >150 Pa): cells become distorted in such a way that their membrane collapse upon themselves. Shear stress > 150 Pa represents the threshold value above which occurs extensive cell damage and high rates of hemolysis are find.

- *Short duration high shear stress* (in excess of 4000 Pa): this hemolysis is caused by the yield stress of the cell membrane being exceeded. In this regime of stress extensive hemolysis occurs.

Considering pressure gradient, Nevaril et al. [43] established that pressure drop of the rate of $\Delta P < 22 \cdot 10^6$ Pa/sec produce little or no red cell trauma.

Table 2.1: Threshold level of $\tau_t >$ in laminar flow for RBCs damage and corresponding estimated exposure time from selected literature

Threshold level of τ_t *(Pa)*	***Order of magnitude of exposure time*** *(s)*	***References***
300	120	Nevaril et al. [43]
150	120	Leverett et al. [38]
150-250	120	Sutera [53]
150	120	Krishna et al. [35]

2.4 Coagulation

Coagulation, or thrombosis, refers to the formation of clots in any part of the system in which blood is circulating. The thrombus lump or clot is an aggregate of blood elements that originates a 3D structure. Thromboembolic conditions are linked to the fluid mechanical properties of blood flow and to the properties of the material of the circuit in which blood flows. Causes can be summed as:

- *Shear stress*: since stress is a natural activator of platelets, during relatively high shear stress, problems like platelets deposition and thrombosis onto biomaterials are of remarkable importance. Platelet activation, and as a consequence stable aggregation, occurs above 8 Pa [26] [42].

- *Shear rate*: the effect of shear rate on coagulation is still under investigation but many studies indicate that low shear rates could promote the initiation of thrombosis by reducing the removal of activated coagulation factors from surfaces. Low shear rates have also been found to increase fibrin deposition, which is a protein involved in blood clotting. Clinically, these hypotheses seem confirmed by the fact that stasis and low blood flow are considered risk factor for vein thrombosis. Moreover, at very

low shear rate conditions, such as those associated with stagnations zones, the fluid shearing forces of blood are not sufficient to overwhelm the forces associated with cell-cell interaction, so that, stable interaction between blood cells can be observed in these low shear environments. Investigations on the existence of a shear rate threshold value for the presence of coagulation have led Hirsch et al. [30], in 1968, to suggest $\dot{\gamma} \simeq 46 sec^{-1}$ as a lower limit for the absence of coagulation. Recent studies carried out by Shen et al. [50] propose a threshold of $\dot{\gamma} \simeq 20 sec^{-1}$.

- *Surface contact*: all surfaces other than the undamaged vascular wall endothelium induce a sequence of processes that results in thrombus formation. When blood comes in contact with a foreign material, such as biomaterials, the first clinically manifest process that occurs is the activation of haemostasis. The study of this contribute lie outside the scope of this thesis and, as a consequence, in the next studies it won't be considered.

Chapter 3

Bellco's Monitor and Bloodlines state of the art

This chapter traces an introduction regarding Bellco's hemodialysis machine and bloodlines that are currently produced and commercialized. In the final section, considerations that led to re-design of the disposable 'Cassette' are described.

3.1 Hemodialysis machine

A 'hemodialysis machine' or 'monitor' is a device that allows a dialysis treatment to be carried out once the functional parameters are defined. Generally, the tasks of a hemodialysis machine are:

- to convey blood to the filter and returns it to the patient;
- to provide for the supply of dialysate;
- to adjust the fluid exchange between blood and dialysate;
- to verify the proper running of a treatment by monitoring given variables (i.e. blood and dialysate pressures inside lines);
- to monitor the effectiveness of treatments;

Dialysis treatments in extra-corporeal circuit can be performed with different kinds of monitors. It is possible to operate a distinction as schematically shown in Figure 3.1.

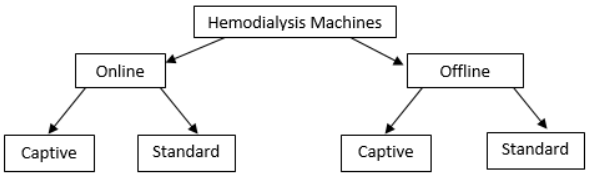

Figure 3.1: Distinction between the different type of monitors

Both on-line monitors and off-line monitors exist; this division is based on the production method of the dialysate. In short, an on-line monitor is directly connected to the feedwater wastewater pipes of the host building in which is located and is provided with internal circuits and ultrafilters able to generate the dialysate. An off-line monitor uses pre-filled bags of fresh dialysate and empty bags to drain the spent dialysate. The second differentiation is between Captive and Standard monitors. A Captive hemodialysis machine is able to carry out a treatment only via a custom disposable device specific for that model: dialysis is carried out only if the monitor recognizes the form of the device. A Standard monitor performs dialysis treatment using disposable device with a standard layout marketed by any manufacturer (device's structure must be compatible with the pressure reading tools of the monitor).

Bellco's hemodialysis machines differ according to the type of patient to treat:

- *Acute Patients*:
  - Amplya® (Offline, Captive): it is a multitherapeutic system for critical care capable of performing a vast number of extracorporeal blood treatments with one single circuit. For each specific disease, Amplya® offers an integrated and personalized therapeutic approach that can aid patient survival and improve their quality of life.
- *Neonatal Patients*:
  - Carpediem® (Offline, Captive): smaller patients have until today not been able to count on personalized treatments,

especially with regard to fluid balance. Carpediem® is the only device on the market that offers specific neonatal treatments: miniature and portable, it responds to the safety and efficacy requirements for renal replacement therapies in such patients.

- *Chronic Patients*:
  - Formula® (Offline, Standard): it was mainly used until the introduction of the monitor Flexya® in 2012.
  - Flexya® (Online, Captive): it is a monitor that allows administering the largest possible number of dialysis treatments, so as to offer to each patient the best possible therapy.

Monitors 'Amplya®' and 'Flexya®' interface with the Captive disposable device examined in this thesis work. For that reason, Figure 3.2 shows, as example, the monitor 'Flexya®' and its main components. Numbered components are listed in Table 3.1.

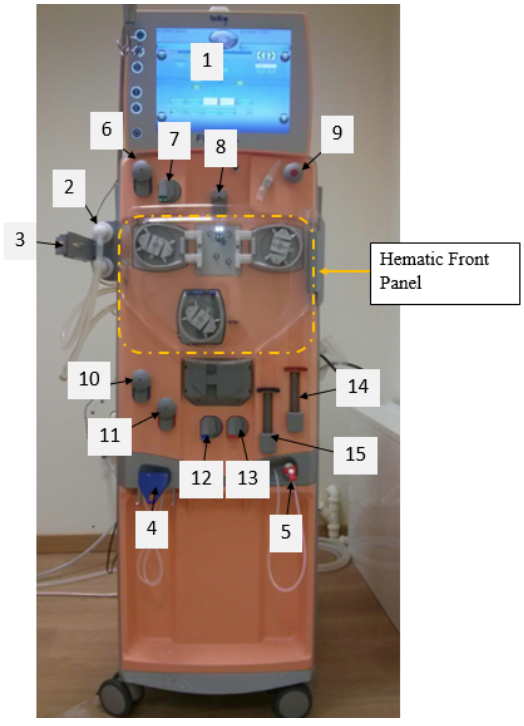

Figure 3.2: Front view of Bellco's monitor Flexya®.

Table 3.1: List of Flexya®'s Components

Number	*Corresponding Component*
1	Display
2	Dialysate connectors
3	Gripper for dialyzer positioning
4	Bicarbonate connector
5	Acid solution connector
6	Connector for dialysate infusion
7	Infusion line clamp
8	Level detector
9	Potentiometer
10	Connector for venous bloodline
11	Connector for arterial bloodline
12	Venous line clamp
13	Arterial line clamp
14	Heparin pump
15	Heparin pump

The frontal hematic panel is made up of (zoomed in Fig.3.3):

- *Peristaltic pump*: designated for the generation of fluxes, they are distinguished in arterial pump, venous pump and infusion pump;
- *Actuator-Sensor 'Cassette Group'*: pressure sensors, cassette's latching and locking mechanism, disposable identification camera.

3.2 Bloodlines currently in use

Once the main component and function of a hemodialysis machine have been described, it is worth noting that, in order to perform a dialysis treatment, they have to be connected to the bloodlines (hemodialyzer and disposable device). The next paragraphs describes with Bellco's bloodlines main components and functions.

3.2.1 Dialyzer

The dialyzer is the central component of the hemodialysis system: blood purification, that is the goal of a dialysis treatment, occurs in-

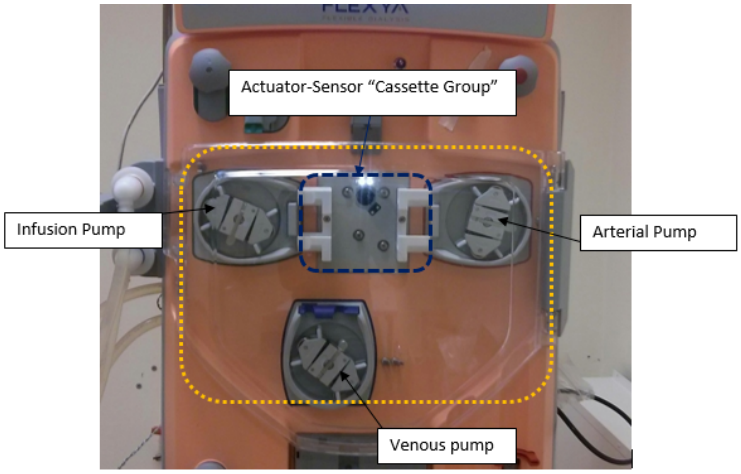

Figure 3.3: Flexya®'s frontal hematic panel.

side it. The blood compartment of the dialyzer is no longer monolithic nowadays, rather it is composed of thousands of semi-permeable capillaries (diameter of about 200μm) called 'fibres'. Blood and dialysate flow on the two sides of the semi-permeable fibers in a countercurrent manner. It is the dialyzer membrane (formed by the fibres) that basically decides which molecules are retained in the blood stream and which diffuse to the dialysate side: several kind of filters exist which are based on this membrane filtering characteristic. Dialyzers differ in their dimensions and number of fibres. In turn, fibres differentiate depending on the material with which they are manufactured (polyethersulfone, poly-amide, polymethylmethacrylate and other) and on the size of their pores. A complete dialyzer is made up of the fibres bundle inserted into a cylindrical plastic case (see Fig.3.4).

Bellco's dialyzers contain from $\sim$ 5000 to $\sim$ 12000 fibres made of polyethersulfone and, based on the size of the membranes' pores, are distinguished in High-Flux and Low-Flux. The cylindrical plastic case is made of polycarbonate (a polypropylene alternative is under development, see Fig.3.6).

In order to ensure and adequate purification of blood, typical blood fluxes are of the order of $300mL{\cdot}min^{-1}$, dialysate flux of $500mL{\cdot}min^{-1}$.

Figure 3.4: Typical Bellco's dialyzer; indicated blood inlet and outlet, dialysate inlet and outlet.

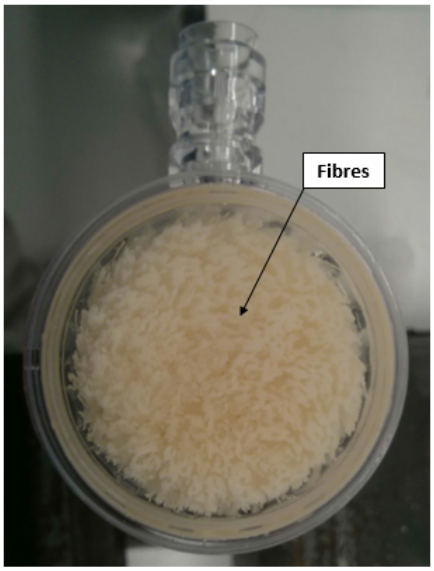

Figure 3.5: Example of uncapped dialyzer.

3.2.2 Cassette

Prior to the release of the monitor Flexya® in 2012, the bloodline was very simple and composed of separated arterial and venous lines, each provided in a separate blister. Furthermore, the monitor-bloodline coupling only allowed the implementation of standard treatments. Until 2012, Bellco's hemodialysis machine for chronic patients was the monitor 'Formula®' (of which many variations exist) and an example of its bloodline for a standard bicarbonate dialysis (BHD) is shown in fig.3.7. This kind of monitor-bloodline coupling presents the following limitations:

- impossibility to perform customized treatments, specific to the needs of the patient;

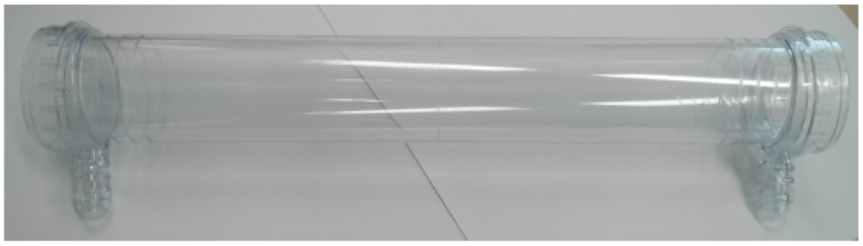

(a) Polycarbonate case.

(b) Polypropylene case.

Figure 3.6: Plastic case of dialyzer

- bloodlines assembly requires time and manual dexterity of the operator.

In order to remove these disadvantages and because of the need to develop new products to penetrate the market, in 2012 the monitor Flexya® was introduced. For the purpose of executing a dialysis treatment, Flexya® makes use of a bloodline characterized by the presence of the cassette. Thanks to this new monitor-cassette coupling, the following requirements of the marketing division have been satisfied:

- execution of 14 different kinds of treatment, customized to patient's needs;
- quick and automatic bloodline installation on the monitor (improved ergonomics).

The Flexya® hemodialysis machine has already been analyzed in sec.3.1. Here the disposable is considered, which consists of:

- *Cassette*: the component that interfaces with the hematic frontal panel of the hemodialysis machine;
- cuvette (hematocrit measuring instrument);

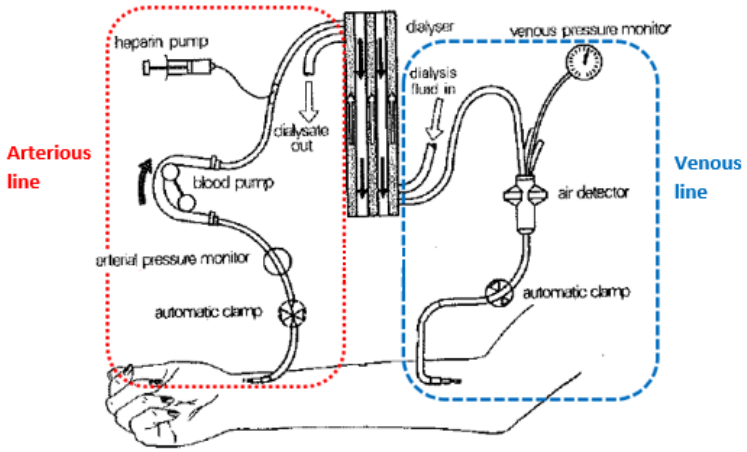

Figure 3.7: Example of BHD standard Formula® bloodline.

- connectors;
- tubes (arteriosus line, venous line, infusion line).

The component of interest in the following is the *cassette*. The cassette is a 5 cavities device, made of rigid thermoplastic material, that can be schematized as in Fig.3.8.

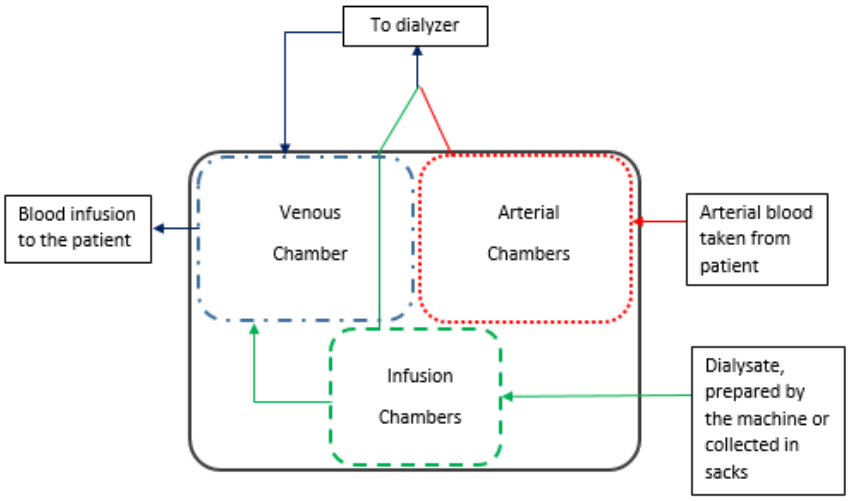

Figure 3.8: General schematic of the 'Cassette'. 'Arterial' means 'before dialyzer', 'venous' stays for 'after the dialyzer'.

The operating principle of the cassette can be understood referring to the arrows of Fig.3.8 that indicates the direction of the fluxes circulating inside the device: blood is drawn from the arterial access of the patient, enters the arteriosus compartment of the cassette and thanks to the movement of the arterial peristaltic pump is directed to the dialyzer. Contemporary, dialysate is also drawn by the infusion pump and directed to the hemofilter for the pre-dilution. Once filtration has been carried out, the cleansed blood enters the venous chamber together with the dialysate flux generated by the venous pump for the post-dilution and from here returns to the patient.

More exhaustively, the functions of the cassette are:

- blood and dialysate directioning;
- monitoring of blood and dialysate pressures during dialysis treatment;
- deaeration of blood.

Cassette's functions are carried out through the five cavities highlighted with letters in Figure 3.9:

Chamber A is the **Arterial pre-pump** blood chamber: fistula[1] pressure measurement in order to monitor the effectiveness of pumping, within the following range:

- Range: (-400; +200) mmHg;
- Maximum rating: (-400; +400) mmHg;

Chamber B is the **Arterial post-pump** blood chamber: pre-dialyzer pressure measurement in order to monitor the absence of clogging in the dialyzer, within the following range:

- Range: (-200; +800) mmHg;
- Maximum rating: (-400; +800) mmHg;

[1] *Fistula*: a type of vascular access for hemodialysis that consists in an artificial communication, obtained via surgery, between an artery and a vein, in order to divert high pressure arterial blood in the venous system so as to obtain adequate blood flow to carry out dialysis treatment [11].

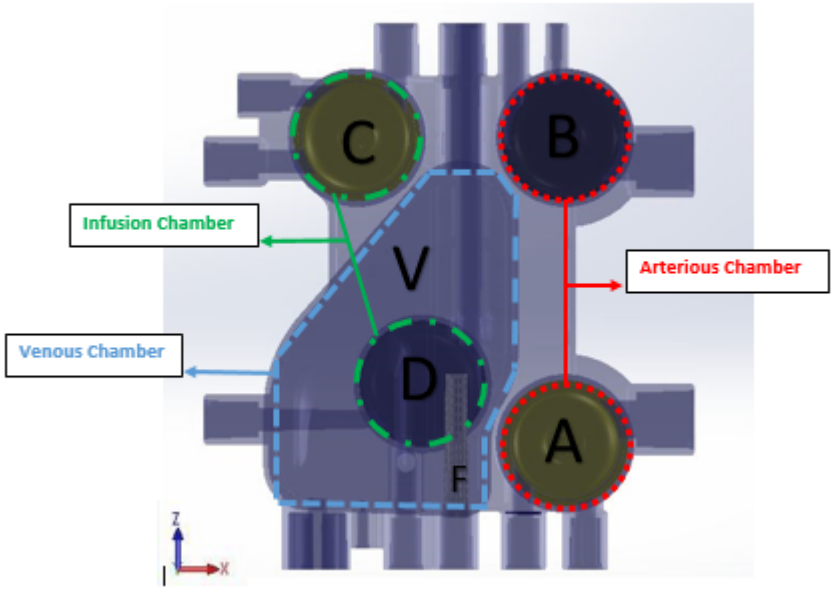

Figure 3.9: CAD model for the cassette; letters indicate the various chambers

Chamber C is the **Infusion chamber**: infusion negative pressure measurement in hemodiafiltrative treatments, within the following range:

- Range: (-400; +200) mmHg;
- Maximum rating: (-400; +800) mmHg;

Chamber D is the **Infusion chamber**: infusion positive pressure measurement in hemodiafiltrative treatments, within the following range:

- Range: (-200; +800) mmHg;
- Maximum rating: (-400; +800) mmHg;

Chamber V is the **Venous chamber**: allows blood deaeration and enable venous infusion pressure measurements in order to monitor to absence of clots, within the following range:

- Range: (-200; +500) mmHg;
- Maximum rating: (-400; +500) mmHg;

Note that letter **F** in the Venous chamber indicates a small filter that prevents the infusion to the patient of any impurities or clots.

Chambers A,B,C,D are used to monitor pressure during treatments. Monitoring is paramount in order to achieve the maximum effectiveness of dialysis: during a dialysis session, pressures must oscillate within specific ranges. Pressure transduction is committed to concave, disc-shaped, impervious membranes (see Fig.3.10) that divide the respective chambers in two hermetically separate compartments: one contains liquid (blood/dialysate) while in the other there is trapped air that serves as control volume for the transducer (see Fig.3.11). Depending on the pressure variations of the liquid in the respective compartment, the membrane is stimulated to deform and transmit the pressure oscillations to the air control volume. This sequence liquid-membrane-control volume represents the pressure transduction pathway (see Fig.3.12).

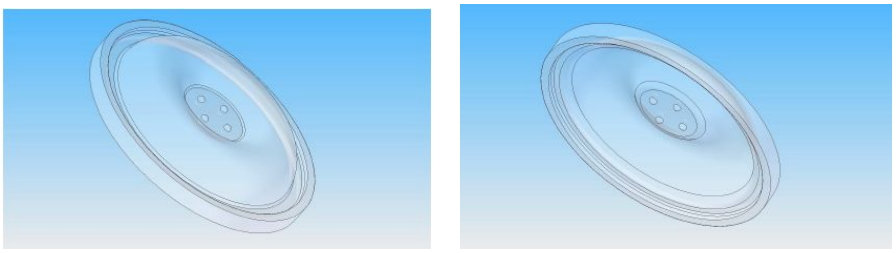

(a) Top view of membrane. (b) Bottom view of membrane.

Figure 3.10: Schematic of a membrane [22].

Depending on the type of measure (higher of lower that the preload-pressure, that is equal to the atmospheric pressure), the membrane must be placed with the concavity towards liquid compartment (negative pressure measurements) ot toward the air compartment (positive pressure measurements), as summed in Fig.3.13 and Fig.3.14.

As mentioned before, the venous chamber 'V' is the only whose main purpose is not just pressure monitoring. In fact, it makes deaeration of blood possible. This function is paramount for patient safety. During dialysis treatments, microemboli develop in the blood circuit: if they are not trapped in the venous chamber, they can be returned to patient's vascular access (in the worst case, embolism can result in patient death in the event that it affects an artery). Downstream the

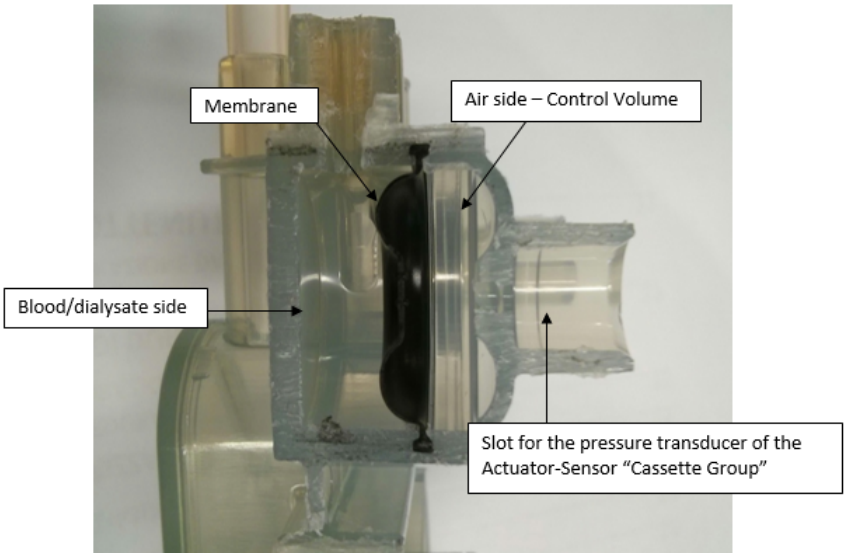

Figure 3.11: View of a sectioned chamber used for positive pressure measurements.

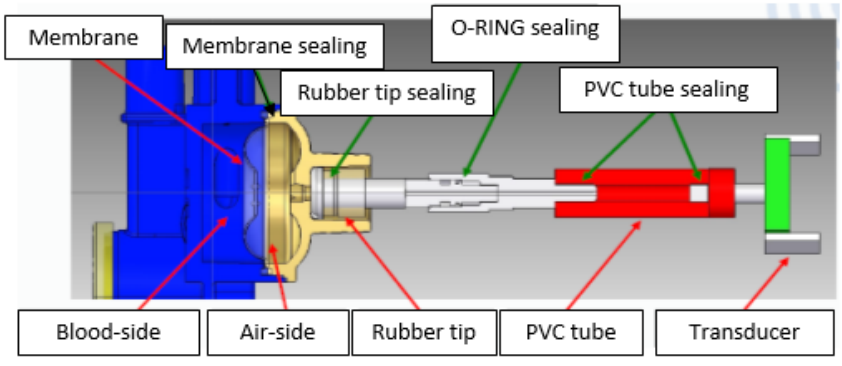

Figure 3.12: Layout of the pressure transducion sequence [20].

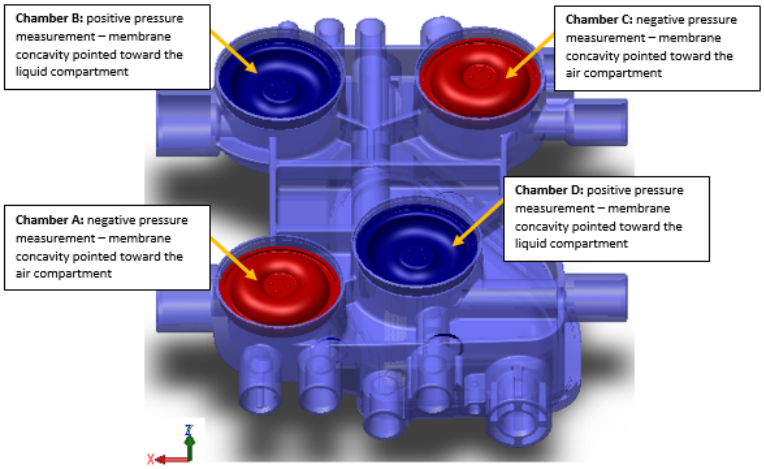

Figure 3.13: View of the correct placement of membranes inside cassette

Figure 3.14: Membranes positioning in chambers.

venous chamber a supplementary air detector and a clamp are provided as an additional safety measure.

Once cassette's components and relative functions have been defined , the currently used cassette is shown (Fig.3.15).

The materials of which i is made of are summarizeed in tab.3.2;while Fig.3.16 and Fig.3.17 show its body and membranes respectively.

Table 3.2: Currently used materials

Component	***Material***
Cassette's body	PVC
Membranes	EPDM

PVC (polyvinyl chloride) is a biocompatible[2] plastic material commonly used for the fabrication of medical disposable. Its main advantages are:

- low cost;
- moulding and bonding ease;
- possibility to modulate its mechanical properties by adding additives during the extrusion process (in the past, the most commonly used additives - plasticizers - were phthalates, ever since banned for their toxicity, nowadays the more stable and non-toxic terephthalates are used).

PVC does not possess good mechanical properties, thus, larger thicknesses are required in order to manufacture rigid components. Larger thickness may cause problems in moulding and cooling of the parts. Another unfavourable feature of PVC is its yellowing caused by sterilization or ageing. For obvious reasons, yellow is not a likeable color for a medical disposable: for that reason the currently used cassette is doped with brighteners (antagonists to the yellow degradation products).

[2] *Blood Compatibilty*: when in contact with a living system, the material must not cause adverse reactions that can compromise the ability to use it for as long as expected. Especially, an essential requirement for a haemocompatible material is its non-thrombogenicity (must not encourage the formation of clots when in contact with blood) [66].

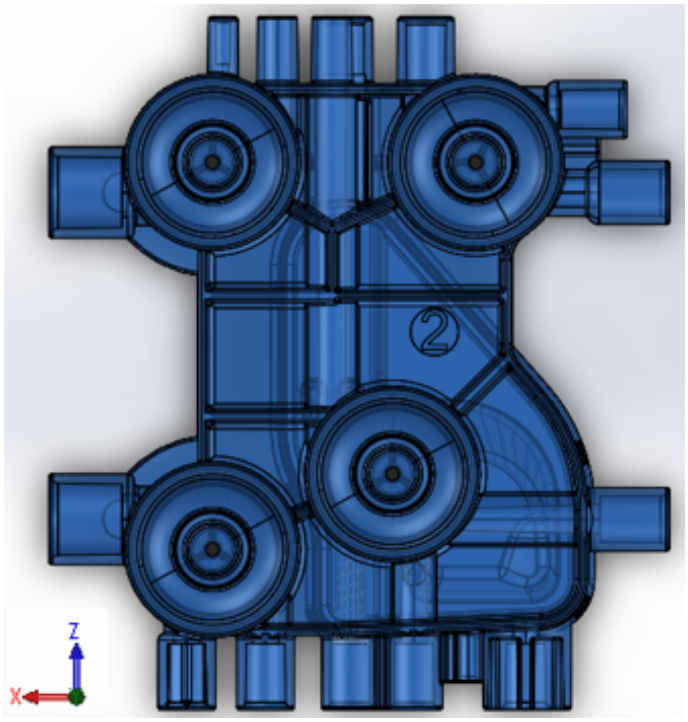

(a) Front view.

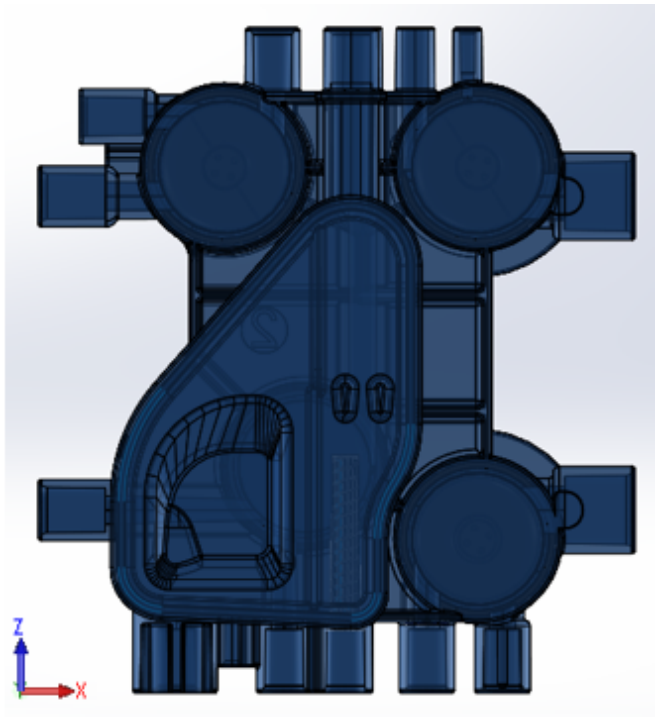

(b) Rear view.

Figure 3.15: View of currently used cassette.

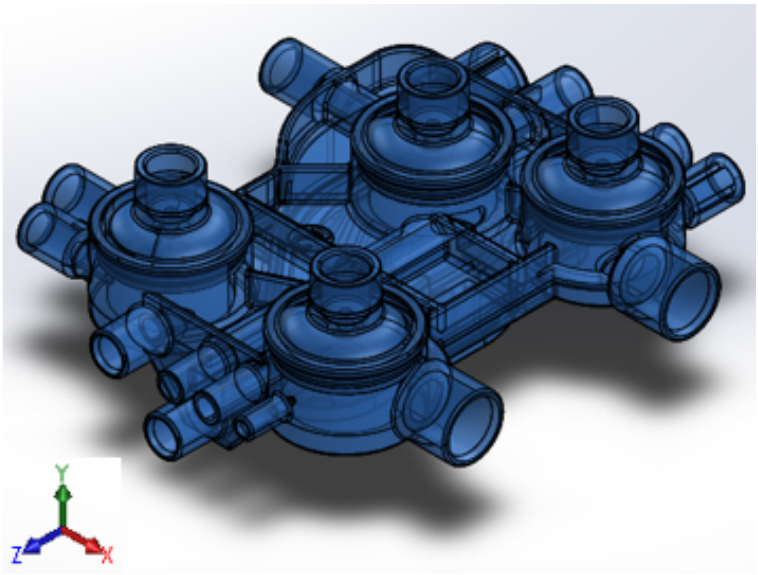

(c) Isometric view.

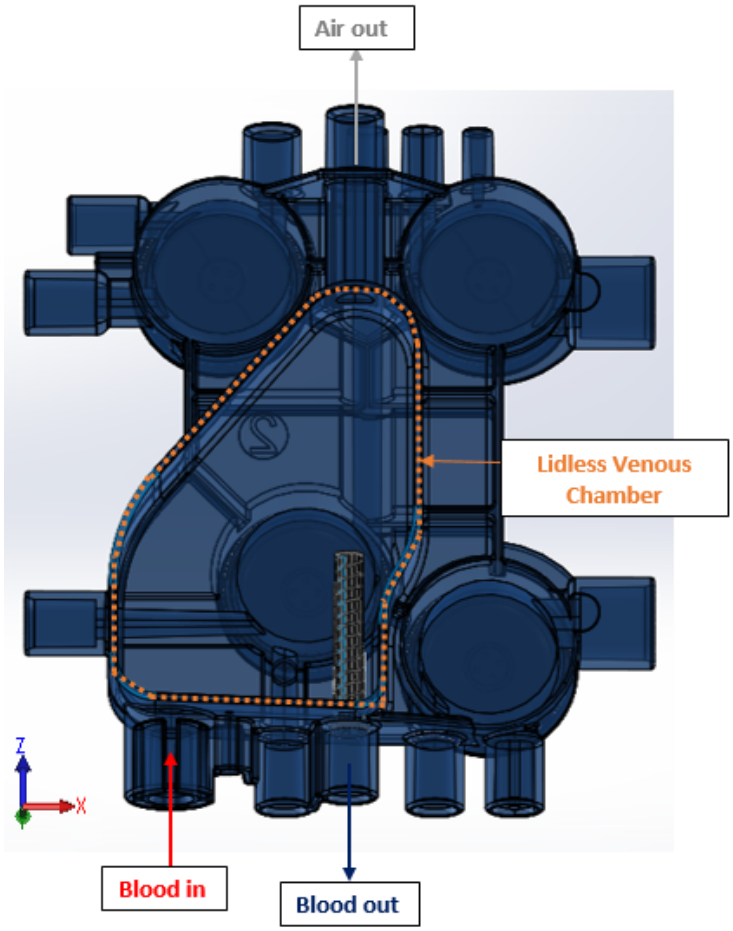

(d) Venous Chamber detail.

Figure 3.15: Views of currently used cassette.

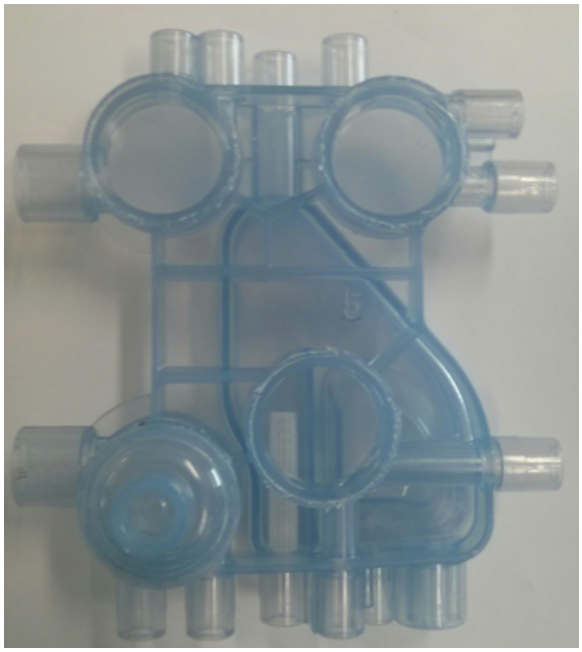

(a) Front view of the PVC cassette's body.

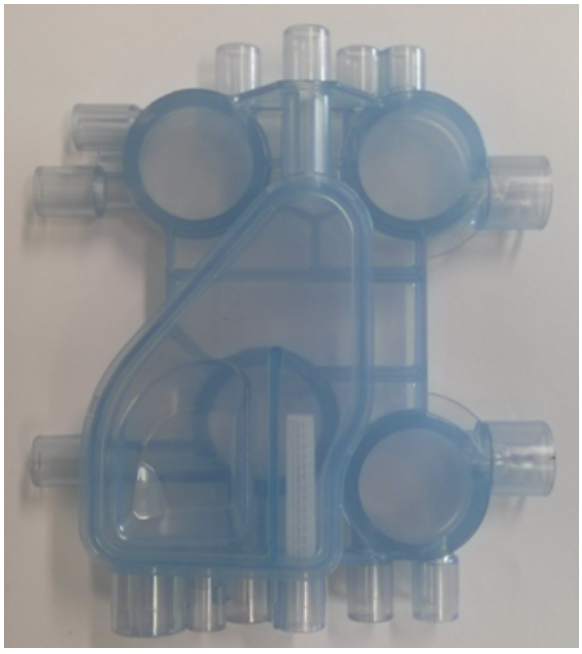

(b) Rear view of the PVC cassette's body.

Figure 3.16: PVC cassette's body.

EPDM is a thermosetting elastomer made of ethylene, propylene and a diene monomer. It is a haemocompatible material, suitable for blood contact, characterized by good mechanical properties and gas impermeability. An unfavourable characteristic is its black colour.

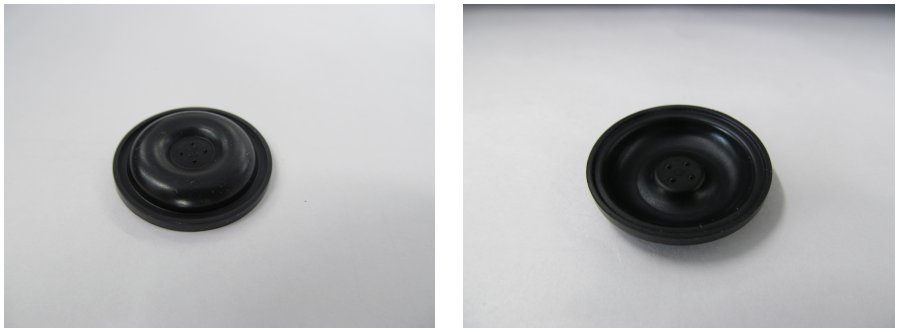

(a) Top view of EPDM membrane. (b) Bottom view of EPDM membrane.

Figure 3.17: EPDM membranes.

3.2.3 New Cassette's Design Input Requirements

In the previous section, components and respective functions of the currently used cassette and the materials with which it is manufactured have been described. Moreover, the main advantages and disadvantages of both the PVC cassette's body and the EPDM membranes were highlighted. In the following section, the motivations that led to the design of a new disposable, which are mainly linked to the choice of new materials, are listed. They can be summarized as follows:

- **reduction of manufacturing costs and time**: the productive process of the currently used cassette consists in molding for the PVC cassette's body and molding followed by vulcanization for the EPDM membranes. These processing techniques, together with part assembly, do not ensure process repeatability and robustness and, furthermore, are characterized by high production costs and times. As will be seen in the next chapter, in order to fulfil this input, new materials that allow co-moulding have been chosen: this guarantees lesser production costs and times and major robustness of the production process;

- **specific requirements for the new materials**: chosen polymers selected for the replacement of PVC and EPDM should have similar mechanical properties, must be haemocompatible and they must be transparent. All these properties must be fulfilled even after sterilization (with beta or gamma ray) and ageing;
- **disposable's rigidity improvement**;
- **design manufacturing improvement**;
- **better removal of entrapped air**: deaeration of circulating blood is paramount both for patient safety and for a proper execution of the treatment;
- **removal of elements that promote coagulation**.

Chapter 4

Cassette New Design

In sec.3.2.2, components and main functions of the disposable were examined. The one currently used was also shown and described. In this chapter the new design of the cassette is presented and choices that were made in order to satisfy the project inputs are clarified.

4.1 Geometry

First of all, it must be made clear that changes to the geometric layout of the new cassette are limited by constraints imposed by the interface between cassette and monitors. These constraints, illustrated in Fig.4.1, are represented by:

- *Constraints A*: mutual positioning between the slots of the pumping segment;

- *Constraints B*: mutual positioning between the slots of the pressure transducer of the monitor.

Moreover, the new cassette must have the same number of ports (16, as shown in Fig.4.2), in order to allow the implementation of all feasible the treatments with the cassette currently used.

Figures 4.3 shows the layout of the new cassette.

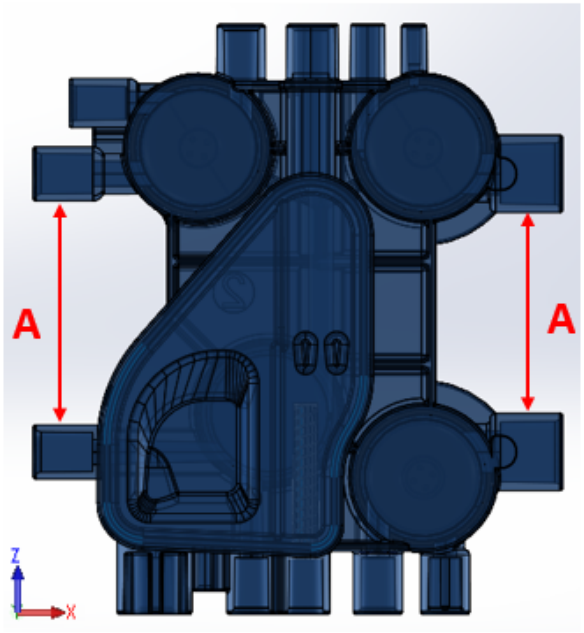

(a) Constraints A.

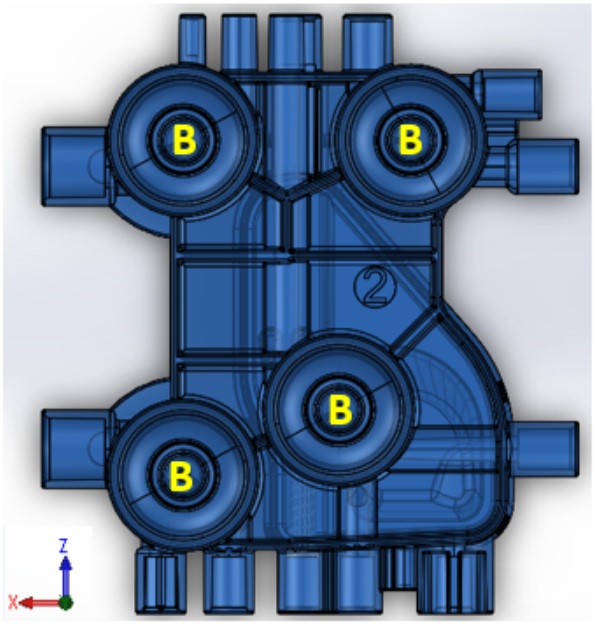

(b) Constraints B.

Figure 4.1: Currently used cassette; constraints indicated with letters.

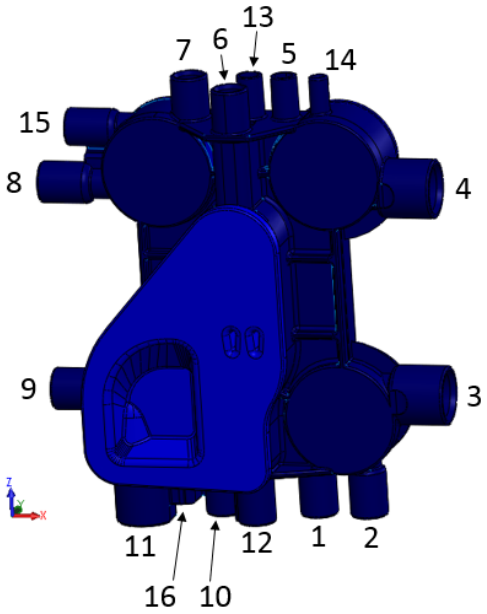

Figure 4.2: Currently used cassette; ports indicated by numbers.

4.2 Materials

The project inputs for the design of the new cassette mainly concern the choice of the materials of which the cassette and the membranes are manufactured. The fulfilment of the requirements explained in sec.3.2.3 led to the following choices.

- **Cassette's body**: to replace PVC, the polymer PETG SKYGREEN S2008 was chosen (see Fig.4.4). PETG is obtained from PET (polyethylene terephthalate) by addition of a glycol. This results in improved workability, allowing the moulding of significantly complex parts too. Furthermore, compared with the PET, PETG melts more easily and shows less crystallization, resulting in lower fragility, lower shrinkages but also in reduced resistance.

  The strengths of PETG to PVC are:

  - possibility of being co-moulded;
  - excellent mechanical properties allowing lower thickness;

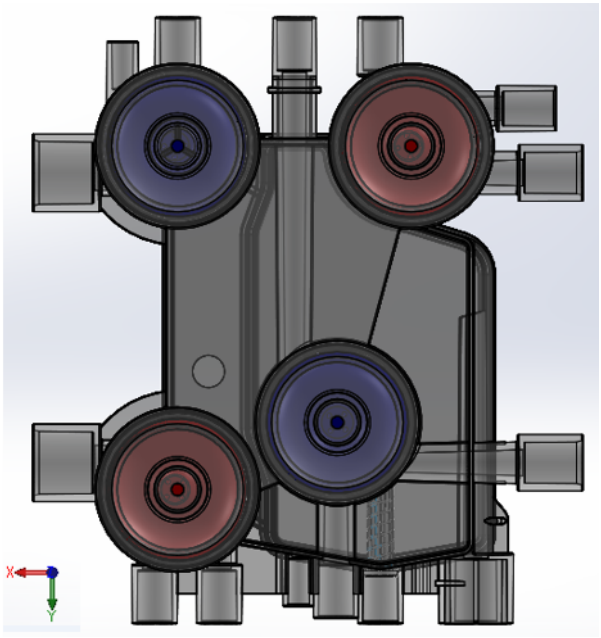

(a) Front view.

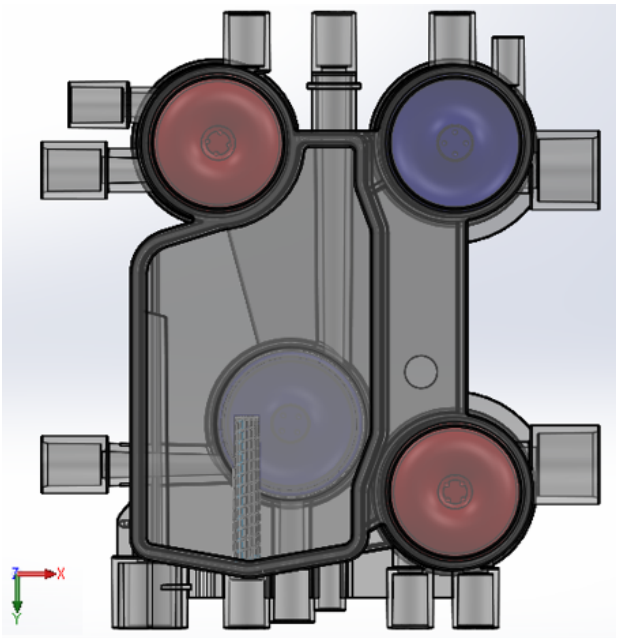

(b) Rear view.

Figure 4.3: View of the new cassette.

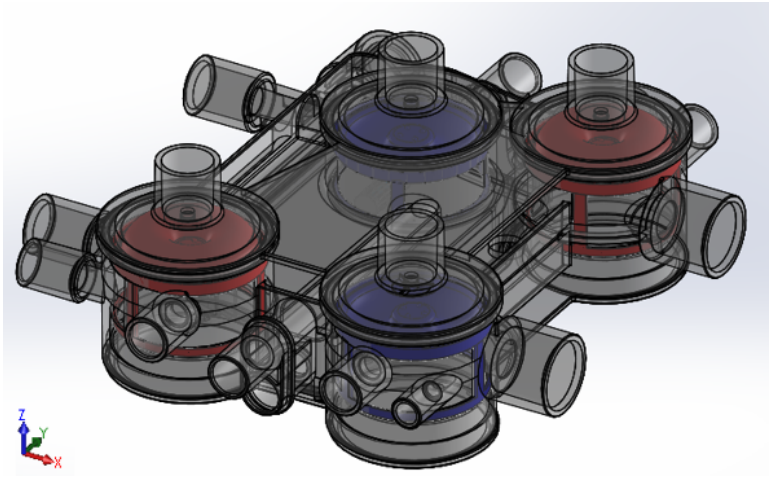

(c) Isometric view.

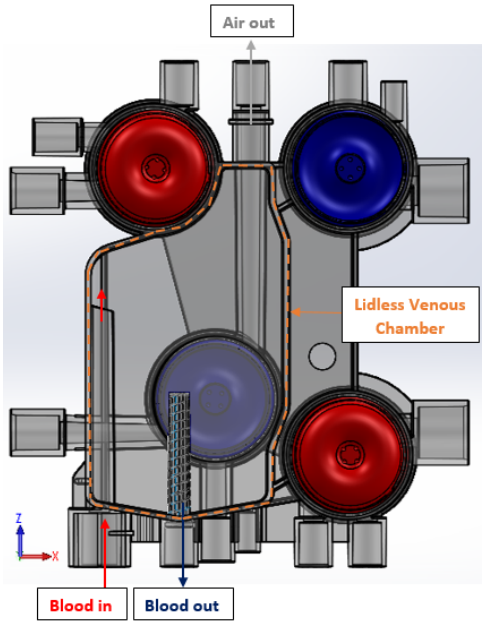

(d) Venous Chamber detail.

Figure 4.3: Views of the new cassette.

(a) Front view.

(b) Rear view.

Figure 4.4: Photos of the PETG cassette.

- high softening temperature allowing fast moulding (PETG does not require long cooling times);
- excellent clarity and haze;
- PETG does not need the use of brighteners since it does not turn yellow as a result of sterilization or ageing.

On the other hand, disadvantages of PETG in comparison to PVC are:

- higher cost of raw material (abated by the possibility of co-moulding);
- bonding problems with tubing due to its resistance to cyclohexanone.

- **Membranes**: concerning the replacement of EPDM, a PE elastomer manufactured by the German company 'ACTEGA'was chosen (see Fig.4.5). This elastomer has slightly worse mechanical properties than the EPDM, but can be manufactured with co-moulding and it is transparent (even after sterilization and ageing). In addition, experimental tests conducted in the company laboratories have proved its satisfactory reliability and accuracy as a pressure transducer.

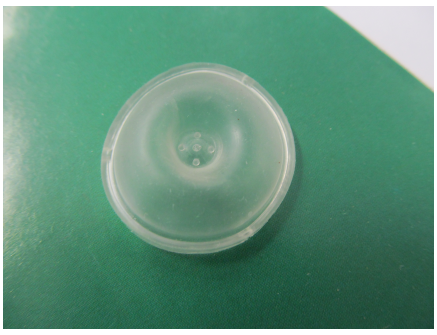

(a) Top view of the ACTEGA membrane.

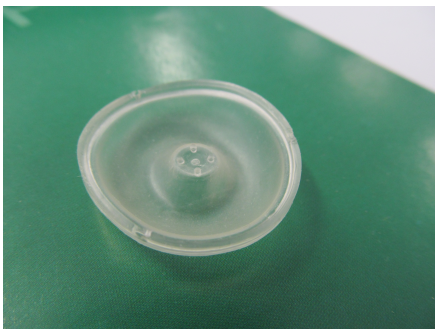

(b) Bottom view of the ACTEGA membrane.

Figure 4.5: ACTEGA membrane.

In summary, according to the project inputs requirements, the new cassette shall be co-moulded and shall be produced faster that the

one currently in use. It shall also be lighter and at the same time less deformable, it shall be transparent and will not turn yellow. It is also worth noting that the new disposable is characterized by colour uniformity (see Fig.4.6), guaranteed by the transparency of both the PETG-SKYGREEN and the elastomer-ACTEGA, unlike the currently used ones (light blue PVC - black EPDM).

4.3 The Venous Chamber

The venous chamber is the cassette's component that has been changed most, owing to the fact that it should not directly satisfy the constraints A and B (see fig.4.1); its only specifications concerns with the internal volume, which shall not be increased. Changes that have been made, together with reasons that led to their implementation, are summarized below:

a) **external profile modification**: ensures greater rigidity, facilitates molding and ultrasonic welding of the cover;

b) **reduction of the internal volume**: in order to satisfy a request made by the marketing department (the internal volume was decreased from 33,9mm^3 to 27,5mm^3, $\delta V = -23\%$);

c) **relocation of the venous infusion port**: in-vitro tests highlighted that the proximity between the chamber walls and the filer may enhance coagulation; for that reason the venous infusion port, and so the filter, has been relocated in the center of the chamber, where the distance between walls and filter is maximum;

d) **addition of the inlet duct**: its insertion improves fluxes direction and increases recirculation;

e) **bulkhead removal**: its presence caused the occurrence of recirculation zones; it has been removed since now this function is carried out by the inlet duct and in order to decrease the surface that is in contact with blood;

f) **relocation of the heparin infusion port**: molding requirement;

(a) Currently used cassette

(b) New cassette.

Figure 4.6: Differences between colours uniformity in the currently used disposable and in the new ones.

All these modifications are summarized in Fig.4.7 where each letter corresponds to the respective change. In the next chapters, the fluid dynamic efficacy of the new design of the venous chamber is analysed, with the aim of investigating the possible presence of favourable conditions to the occurrence of hemolysis and coagulation.

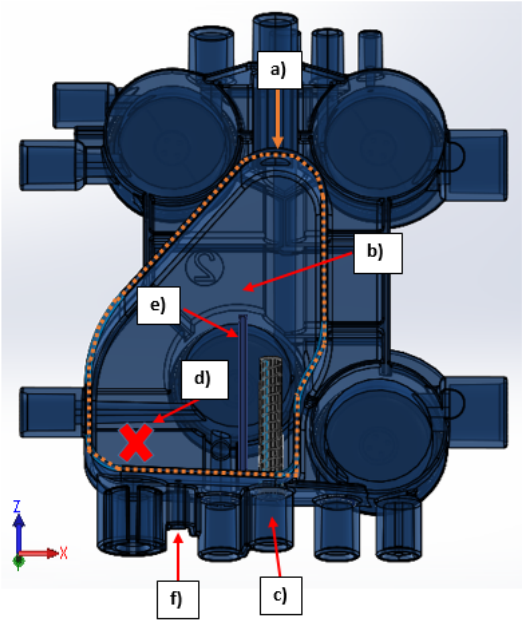

(a) CV of the currently used cassette

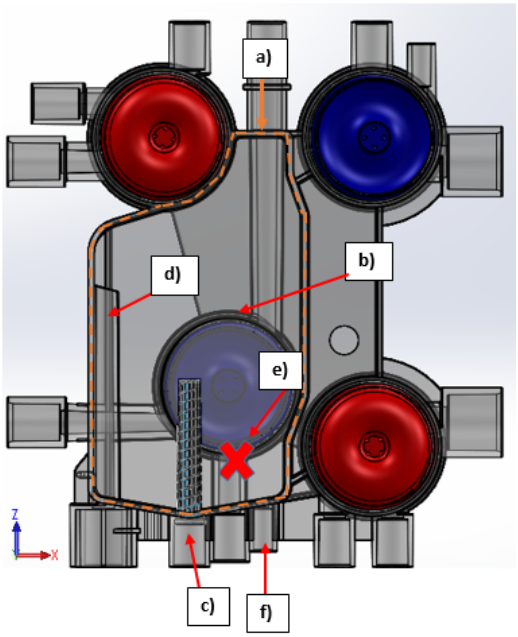

(b) CV of the new cassette

Figure 4.7: Comparison between the venous chambers.

Chapter 5

Numerical Simulations

This section covers the approach of the CFD simulations. The first part contains general theory regarding fluid dynamics (in particular Hemodynamics, which is he study of blood flow in biomechanical systems) and CFD, such as the Navier-Stokes equations, and regarding the Finite Element Method, which is the one employed by COMSOL. The latter part involves the CFD simulations in COMSOL, where the settings are explained in steps and the methods are motivated.

5.1 Hemodynamics

Hemodynamics is the study of blood flow in biomechanical systems. It is a complicated science principally due to the composition of blood (plasma and formed elements) which makes it behave like a non-Newtonian fluid. For many hemodynamics study, approximations are made in order to apply simple fluid dynamics relations to describe blood flows. However, in this thesis blood is considered as an incompressible non-Newtonian fluid. This means that local density variations are neglected but that the shear thinning feature, that is the main non-Newtonian characteristic of blood, is taken into account using the Carreau-Yasuda model.

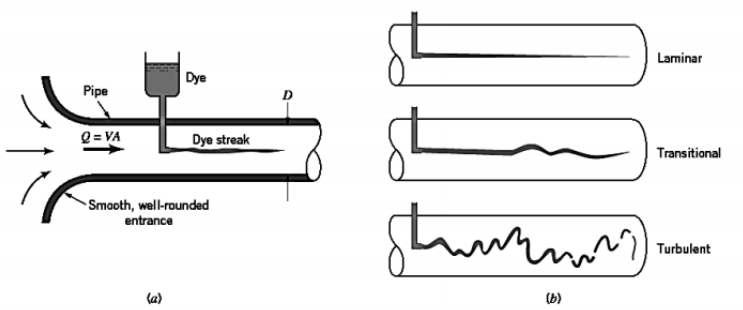

Figure 5.1: (a)Reynolds' experiment using water in a pipe to study transition to turbulence; (b)Typical dye streake [36]

5.1.1 The Reynolds Number

As a natural phenomenon in fluids, the characteristic of the flow can change drastically under certain conditions, for example at high enough velocities. Various quantities can be used to characterize flow in different situations. The Reynolds number is one of these fundamental parameters of the fluid dynamics that allow to mark out the type of flow [10]. This non-dimensional quantity was named after Osborne Reynolds (1842 - 1912) who investigated experimentally (apparatus in Fig.5.1) the transition of flow from the orderly kind that we call 'laminar flow'to the more chaotic type termed 'turbulent flow'. It was known from earlier studies that turbulent flow occurs in conduits of large cross-sectional dimensions and flows at high velocities, whereas laminar flow occurs in slow flows in conduits of relatively small cross-sectional dimensions. The role of viscosity and density in affecting the type of motion was not as well-characterized.

Reynolds established that the change in the nature of the flow occurs when a certain combination of the parameters in the flow crosses a threshold. This combination, that is the '*Reynolds Number*'is defined as follow.

$$Re = \frac{\rho U L}{\mu} = \frac{U L}{\nu} \tag{5.1}$$

where

ρ is the fluid density;

μ is the dynamic viscosity of the fluid;

$\nu = \frac{\mu}{\rho}$ is the kinematic viscosity;

U is the mean velocity of the fluid;

L is the typical length scale of the flow (e.g. the hydraulic diameter for pipe flow).

We can ascribe a certain physical significance to the Reynolds number. This is most conveniently seen by recasting this group after multiplying both the numerator and the denominator by the mean flow velocity U. In fact, this leads to

$$Re = \frac{\rho U^2}{\mu(U/D)} \tag{5.2}$$

In this form, we see that the denominator represents a characteristic shear stress in the flow, because it is the product of the viscosity of the fluid and a characteristic velocity gradient obtained by dividing the average velocity by the diameter of the tube. The numerator, in contrast, describes an inertial stress; recall that the larger the density, the more massive a material is, and mass is a measure of inertia. This is the reason for calling the product ρU^2 a characteristic inertial stress. Thus, we can think of the Reynolds number as the ratio of two characteristic stresses in the flow:

$$Re = \frac{InertialStress}{ViscousStress} \tag{5.3}$$

Stress is force per unit area , therefore it is common to express the physical significance of the Reynolds Number as:

$$Re = \frac{InertialForces}{ViscousForces} \tag{5.4}$$

We see now that the nature of the flow in a tube, whether laminar or turbulent, depends on the relative importance of the inertial forces in comparison with the viscous forces. At low values of the Reynolds number, the viscous forces are relatively more important, and disturbances in the flow are damped out by viscosity. This results in a flow characterized by smooth and organized layer motion. Flow of this kind is said to be in the *laminar* regime. On the other hand, at higher values of the Reynolds number, inertial forces dominate the viscous forces so that the damping of disturbances by viscosity is less effective. This

kind of flow is characterized by the presence of chaotic eddies, vortices and other flow instabilities of widely different length and time scales [58]. In this regime the flow is referred to as *turbulent* and is much more difficult to predict. At moderately high Reynolds numbers, the flow starts changing from laminar to turbulent. This regime is known as the *transitional* regime, where the flow might show characteristic of both laminar and turbulent flow. For a cylindrical pipe, the transition from laminar to turbulent flow usually occurs for Re slightly above 2100 (see Tab. 5.1) but it depends on problem specifics such as surface roughness and geometry variations [55], [36].

Table 5.1: Flow characterization within a pipe by the Reynolds number

Reynolds number	***Flow regime***
Re $<$ 2100	Laminar flow
2100 $<$ Re $<$ 4000	Transitional regime
Re $>$ 4000	Turbulent regime

5.1.2 Velocity Profile

For fluid flow within a pipe, the velocity profile is an important property of interest. The fluid velocity in a pipe changes from zero at the surface because of the no-slip condition (see 5.1.4) to a maximum at the pipe centre. Usually it is convenient to work with an average velocity U_{av}, which remains constant in incompressible flow when the cross-sectional area of the pipe is constant (Fig. 5.2) while in some applications it is necessary to find out the velocity value as a function of the cylindrical coordinates r.

The value of the average velocity U_{av} at some streamwise cross-section is determined from the requirement that the conservation of mass principle (see sec.5.1.3) must be satisfied, that for incompressible fluids in leads to

$$\dot{m} = \rho U_{av} A_c = \int_{A_c} \rho u(r)\, dA_c = const \tag{5.5}$$

where

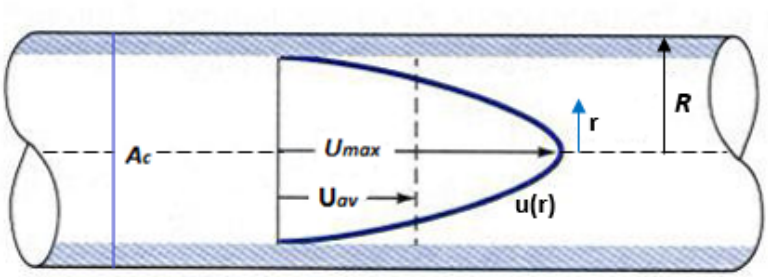

Figure 5.2: Velocity profile within a circular pipe.

ρ is the fluid density;

$\dot{m}$ is the mass flow rate;

A_c is the cross-sectional area;

$u(r)$ is the velocity profile.

The velocity profile, for fully developed laminar flow in a cylindrical pipe with constant diameter, can be derived directly by fundamental principle of fluid flow (Poiseuille flow) and is given by eq.5.6

$$u(r) = 2U_{av}\left[1 - \left(\frac{r}{R}\right)^2\right] \tag{5.6}$$

where

R is the radius of the pipe;

r is the cylindrical coordinates.

This is a convenient form for the velocity profile since U_{av} can be determined easily from the flow rate information. As stated before, the maximum velocity occurs at the centreline and is determined from 5.6 by substituting $r = 0$,

$$U_{max} = 2U_{av} \tag{5.7}$$

Therefore, the velocity profile in fully developed laminar flow in a pipe is parabolic with a maximum at the centerline and minimum (zero) at the pipe wall.

5.1.3 The Governing Equations

The motion of a viscous fluid is governed by the *Navier-Stokes* system of partial differential equations. They are derived by the differential equation of motion combined with the conservation of mass equation. In vector notation, for an incompressible fluid they can be written as

$$\nabla \cdot \bar{U} = 0, \tag{5.8}$$

$$\rho \left(\frac{\partial \bar{U}}{\partial t} + \bar{U} \cdot \nabla \bar{U} \right) = -\nabla p + \rho \bar{g} + \nabla \cdot \left[\overline{\overline{\tau}} \right] \tag{5.9}$$

where
ρ is the fluid density;
$\bar{U} = (u, v, w)$ is the velocity vector;
p is the pressure;
$\left[\overline{\overline{\tau}} \right]$ is the shear stress tensor.

Equation 5.8 is the continuity equation and implies that the mass flux for a volume element must be equal to zero. Equation 5.9 is a set of three equations (one for each dimension) that describes linear momentum conservation. Its left hand side (LHS) represent the acceleration of the fluid, while the right hand side (RHS) describes pressure, viscous stress and other body forces. This system consist of four equations and four unknown variables (*u, v, w, p*), therefore the problem is 'well-posed'in mathematical terms. Anyhow, to fully describe the motion of fluid flow, for a specific problem, the Partial Differential Equations (PDEs) of 5.8 and 5.9 must be complemented with the appropriate boundary and initial conditions.

5.1.4 Boundary conditions

The most common boundary conditions 'BC'are the Dirichlet and the Neumann boundary conditions. The former specifies the values that a variable takes along a boundary while the latter specifies the derivatives of a variable. Common boundaries to fluid flow are the walls confining the fluid and the inlet/outlet boundaries. At the wall we shall require that the tangential component of the velocity of the viscous fluid be zero, which is a result of friction between the fluid and the wall due to

viscosity. This is known as the *no-slip condition*, which is a Dirichlet condition on the velocity:

$$\bar{U}_{wall} = \bar{0} \tag{5.10}$$

Similarly, since there is no mass transfer across the walls, a purely kinematical consequence is that the normal component of fluid velocity, relative to the wall, must be zero there (this represents a Neumann BC):

$$\left.\frac{\partial \bar{U}}{\partial n}\right|_{wall} = 0 \tag{5.11}$$

For CFD simulations, the inlet and the outlet conditions are generally specified by velocity, mass flow rate or pressure. Usually, velocity and mass flow rate conditions are inlet conditions, while pressure conditions are commonly specified at the outlet.

5.1.5 Limitations of the analytical method

The equations of fluid mechanics - which have been known for over a century - are solvable for a limited number of flows only. The known solutions are extremely useful in helping to understand fluid flow but seldom can they be used directly in engineering analysis or design. The governing equations of fluid flow are highly non-linear and impossible to solve analytically for complex geometries, so the engineers have been forced to use other approaches. A alternative or complementary method came with the birth of electronic computers and today, thanks to their ever increasing computing capability it is possible to find solutions for problems that seemed unsolvable. Nowadays, solution of the equations of fluid mechanics on computers has become paramount: this field is known as *computational fluid dynamics* 'CFD'.

5.2 The Finite Element Method

As mentioned in the previous section, flows and related phenomena can be described by PDEs which cannot be solved analytically except in special, simple cases. To obtain an approximate solution numerically, we have to use a discretization method which approximates the differ-

ential equations by a system of algebraic equations, which can then be solved with numerical computation. The approximations are applied to small domains in space and/or time so the numerical solution provides results at discrete locations in space and time. The accuracy of the solutions is dependent on the quality of the discretizations used. There exist many approaches, the most important of which are: finite difference (FD), finite volume (FV) and finite element (FE) methods. This section provide a brief introduction to the finite element method (FEM).

The main idea of the *Finite Element Method* is to divide the domain of the problem into a set of discrete volumes or finite elements which form a grid, and then approximate PDEs locally for each elements . The unknown field variable is expressed in terms of assumed approximating functions within each element of the grid (see Fig.5.3). The approximating functions, also known as interpolation functions, are defined in terms of the value of the field variables at the specified points called nodes or nodal points. Nodes lie on the element boundaries where adjacent elements are supposed to be connected. For the finite elements representation of a problem, the nodal values of the field variable become the new unknowns. Once these unknowns are found, the interpolation functions define the field variable throughout the assemblage of elements.

The many advantage of the FEM is that it doesn't need the grid to be structured unlike FD methods where the mesh elements are of uniform size: this allow to handle very complex geometry too. The downside is that it is mathematically complex compared to other methods such as FV method, another common numerical method often used for fluid flow problems.

5.3 CFD in COMSOL

CFD simulations were run with the software COMSOL Multiphysics® (Version 5.0) and its CFD module. COMSOL is based on the Finite Element Method (see Sec. 5.2), which is well suited for fluid flow problems in complex geometry such as that of the venous chamber

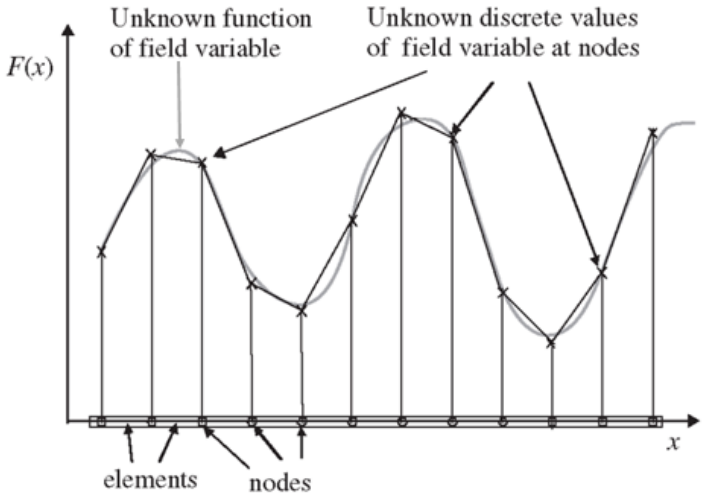

Figure 5.3: Example of 1D finite element approximation; a continuous function is approximated using piecewise linear functions in each subdomain/element [67].

of the 'cassette'. In COMSOL it is possible to create 1D, 2D, 2D-axisymmetric and 3D models, where the geometry, physics (equations and boundary conditions) and the mesh can be defined, all without the need for any additional software. COMSOL also includes various study options (such as solver methods) and post processing alternatives.

5.3.1 Geometry

Given the complex shape of the venous chamber and its lack of symmetry, it was decided to perform simulations using the original 3D geometry (see Fig.5.4), in order to investigate the 3D nature of flow inside it. This results in a substantial increase both in computational cost and process time compared with the use of a 2D geometry but it also allow to obtain a better accuracy in the reconstruction of phenomena such as recirculation bubbles and stagnation points.

5.3.2 Blood Parameters

Blood physical properties for uraemic patients were obtained in agreement with the Scientific Affairs Department (SA Dept.).

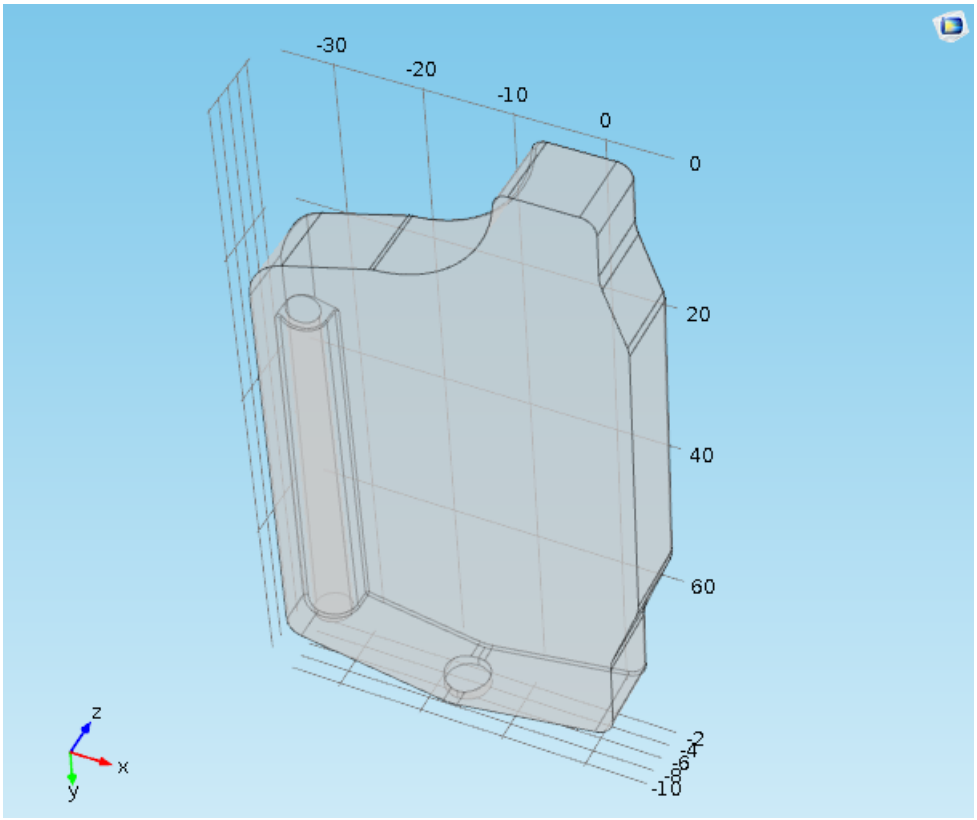

Figure 5.4: Entire geometry of the Venous Chamber.

- *Blood density*: blood density depends on plasma density and hematocrit according to Eq. 5.12, derived from [15].

$$\rho_b = \rho_p \cdot (1 - H) + 1090 \cdot H \tag{5.12}$$

The values of hematocrit and plasma density were suggested by the SA Dept. and are summed in Tab. 5.2. Using that values it

Table 5.2: Values for hematocrit and plasma viscosity for uraemic patients, $T = 37°C$

Parameter	***Value***
H	32 %
ρ_p	1025 Kg/m^3

is obtained

$$\rho_b = 1045.8 \text{ Kg}/m^3$$

- *Blood viscosity*: as stated in Sec.2.2.2, blood acts as a non-Newtonian fluid with shear-thinning property; in order to model blood viscosity the non-Newtonian Carreau-Yasuda model (see Eq.2.3) was chosen (it is already implemented in COMSOL's CFD module). Parameters λ, n, a were obtained from [27], the value of μ_0 was gained from [14] and the value for μ_∞ from [40]. All their values are listed in Tab.5.3 and the resulting graph is shown in Figure 5.5.

Table 5.3: Parameters for the Carreau-Yasuda model

Parameter	***Value***
λ	10.03 sec
n	0.344
a	2
μ_0	0.0384 Pa·s
μ_∞	$4.01 \cdot 10^{-3}$ Pa·s

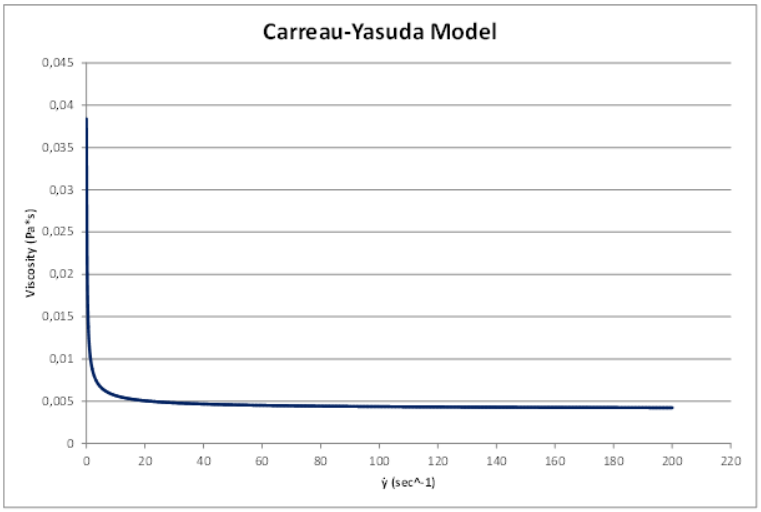

Figure 5.5: Viscosity as a function of shear rate for chosen parameter

5.3.3 Physics and Boundary conditions

COMSOL's CFD module gives the option to model laminar as well as turbulent flow with already implemented physics models. The Reynolds number in the inlet duct was calculated from Eq.5.1 to be below 400, so that the flow is *laminar*. The incompressible Navier-Stokes equations (Eq.5.9) coupled with the corresponding continuity equation (Eq.5.8) were used to solve for the velocity and pressure fields.

The initial and boundary conditions are defined as follow:

- *Initial Conditions*: the initial conditions inside the venous chamber were defined as a zero velocity field and a pressure of 6666 Pa, which corresponds to 50 mmHg, that is a standard pressure value within the venous chamber during a normal dialysis treatment.

- *Inlet Condition*: the available data useful to describe the inlet condition is the volumetric flow rate on the area A_1 (ref. Fig.5.7) that is Q_1=300 $\frac{mL}{min} = 5{\cdot}10^{-6}$ $\frac{m^3}{s}$. In order to simplify the model of the venous chamber, it was chosen to first carry out a simulation of only the inlet duct (highlighted in blue in Fig.5.6 and Fig.5.7) so as to obtain the value of $U_{max,in}$ in the section A_{in}. From this value, using Eq.5.7 it is possible to get the value of the average speed in the section $U_{av,in}$, which is then set as the parameter for the laminar inflow. Moreover, using Eq.5.13 derived from [37], it is possible to calculate the value of the entrance length ($l_{e,lam}$) for laminar flow and Re>50, which is also defined as an inlet BC.

$$\frac{l_{e,lam}}{d} = 0.06 \cdot Re \tag{5.13}$$

  The inlet duct separated from the venous chamber is shown in Fig.5.8. The obtained value for $U_{av,in}$, Re_{in} and $l_{e,lam}$ are summed in Tab.5.4.

- *Outlet Condition*: at the outlet a condition of pressure was set. The pressure value was obtained by experimental tests in dialysis condition and is reported below.

$$P_{out} = 5332Pa$$

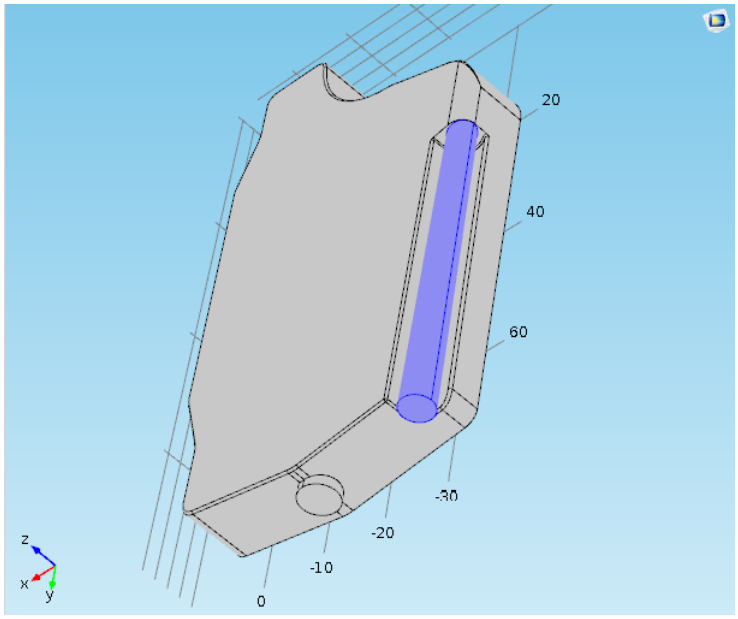

Figure 5.6: Model of the Venous Chamber, highlighted in blue the inlet duct.

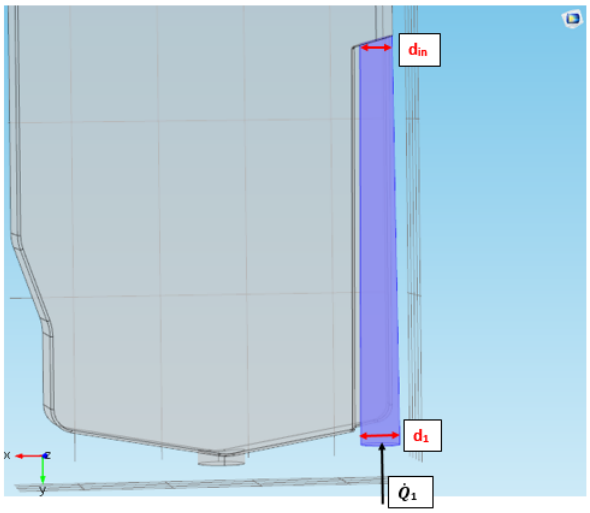

Figure 5.7: Zoom on the inlet duct, indicated sections '1'and 'in'.

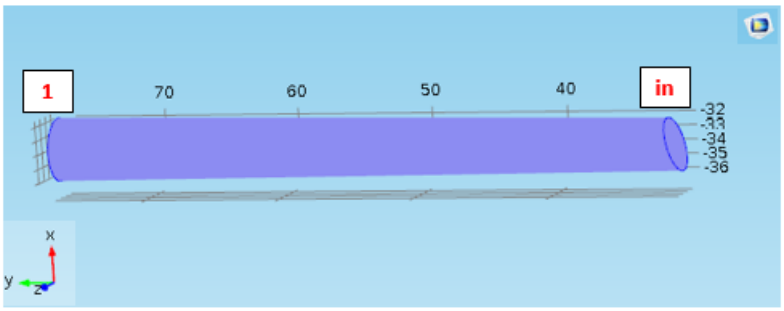

Figure 5.8: Schematic of only the inlet duct.

Table 5.4: Parameters value in section 'in'

Parameter	***Value***
$U_{av,in}$	0.378 m/sec
Re_{in}	366
$l_{e,lam}$	0.1 m

- *BCs at the wall*: for the rigid walls surrounding the venous chamber were set a no-slip condition.

5.3.4 Meshing

A simple free tetrahedral mesh was used. A 2D model mesh analysis was made where the maximum dimension of the mesh elements was decreased with the aim to find a fine enough mesh where no change in a quantity of interest occurred for any additional decrease in the dimension, or until the variations were negligible. The chosen quantity of interest was the y velocity component v evaluated in 16 aligned points at a certain distance from the outlet duct (see Fig.5.9).

As a result of the mesh refinement study data analysis, mesh parameter for the complete 3D model listed in tab.5.5 were obtained.

5.3.5 Studies and post-processing

The CFD studies of the venous chamber of the new cassette aim to verify the effectiveness of its design. According to what was mentioned in

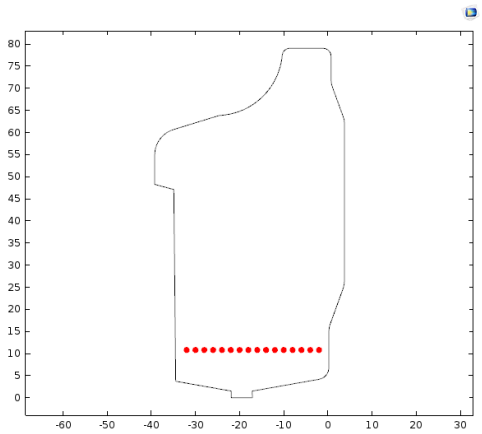

Figure 5.9: 2D model used for the mesh refinement study; red dots represent the 16 points at which the y velocity component was evaluated.

Table 5.5: Chosen mesh parameters

Parameter	***Value***
Maximum element size	0.7 mm
Minimum element size	0.4 mm
Maximum element growth rate	1.45
Curvature factor	0.45
Resolution of narrow regions	0.8

section 2.3 and 2.4, the results obtained from the numerical simulation are analysed with focus on:

1. Presence of a well-streamlined flow and of recirculation zones that limit the presence of stagnation points which promote blood coagulation;

2. Absence of viscous shear stress higher than τ_{pa} ($\tau_{pa} = 8$ Pa): if this condition is satisfied, both platelet activation that facilitate coagulation and shear stress that induce hemolysis are averted;

3. Absence of pressure drop higer than ΔP ($\Delta P = 22 \cdot 10^6$ Pa) that produce red cells trauma;

4. Absence of shear rate lower than the threshold value $\dot{\gamma}_t$ ($\dot{\gamma}_t = 20 s^{-1}$) which favour coagulation.

Chapter 6

Results and Conclusions

In the following chapter, the results obtained from the CFD simulation are reported and discussed, considering their correlation with the functionality of the venous chamber. The final section proposes the conclusion of this thesis work and presents possible future developments that could improve the quality of the results obtained.

6.1 Velocity Field

The results for the blood velocity field can be observed in Figure 6.1 and Figure 6.2. The maximum velocity is obviously found in the centre of the inlet duct and its magnitude is 0.754 m/s. The velocity vectors (red arrows) highlight the presence of a strong flow recirculation, in accordance with our expectations and with preliminary in-vitro tests performed in the company laboratories but not presented in this document. This result is also confirmed by the streamlines shown in Figure 6.3. Figure 6.4 is a close up of the recirculation zone and offers a clearer view of the flows that develop in this area. With regard to the velocity field in the upper zone of the venous chamber, the results obtained are satisfactory. They indicate a well-streamlined flow structure and the presence of recirculation region which introduces fluid mixing. On the other hand, Figure 6.5 highlight the presence, in the lower region, of two zones at low flow speed which must be analysed in depth.

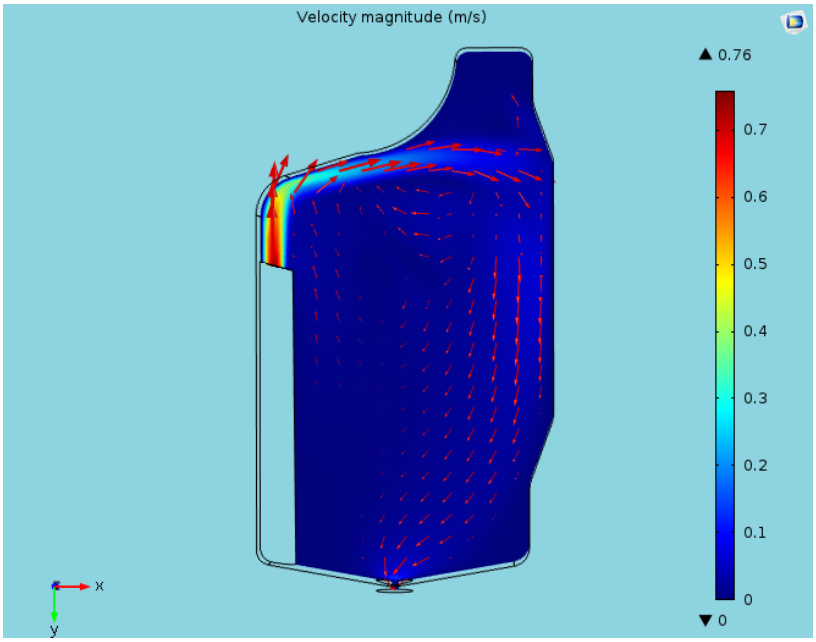

(a) Plane passes through the centreline of the inlet duct.

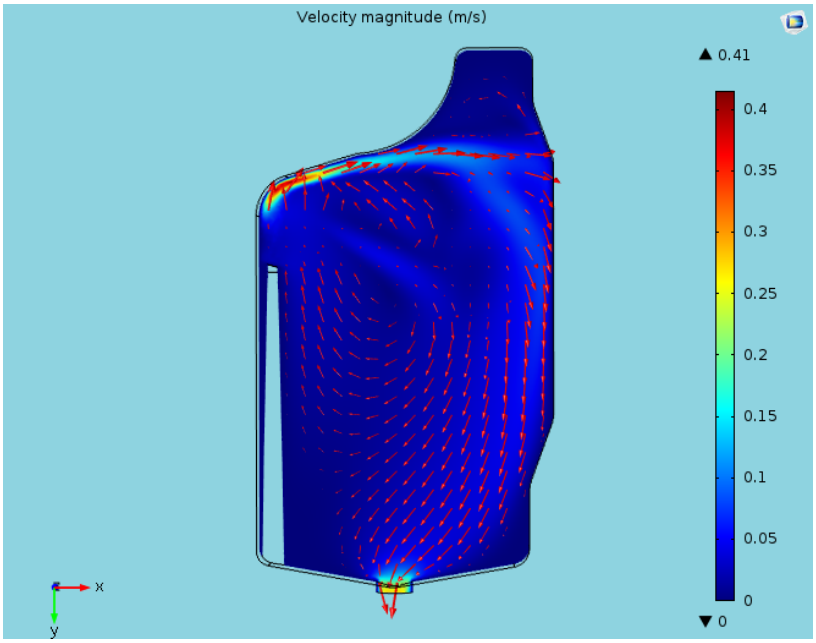

(b) Plane passes through the centreline of the outlet duct.

Figure 6.1: Velocity field profile on x-y planes.

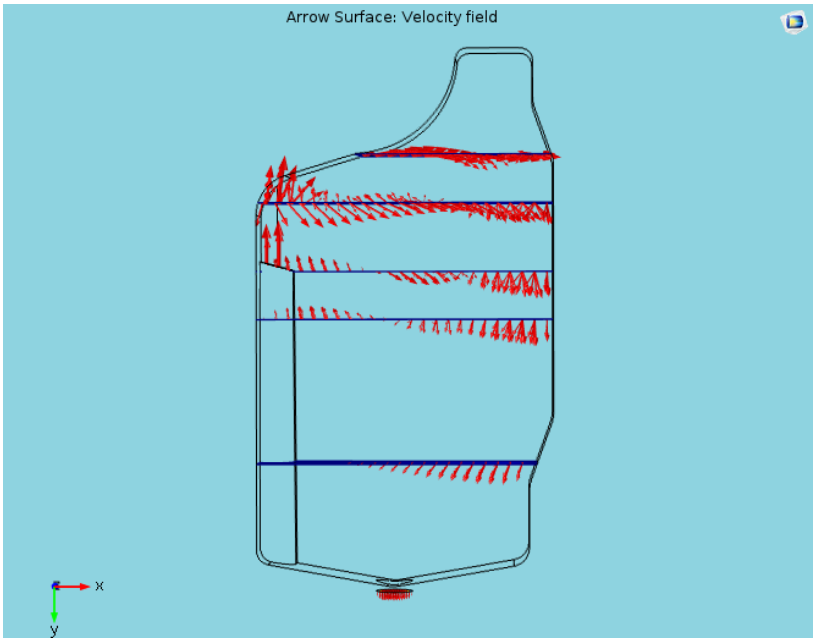

Figure 6.2: Velocity vectors profile on different x-z planes.

Figure 6.3: Streamlines plot.

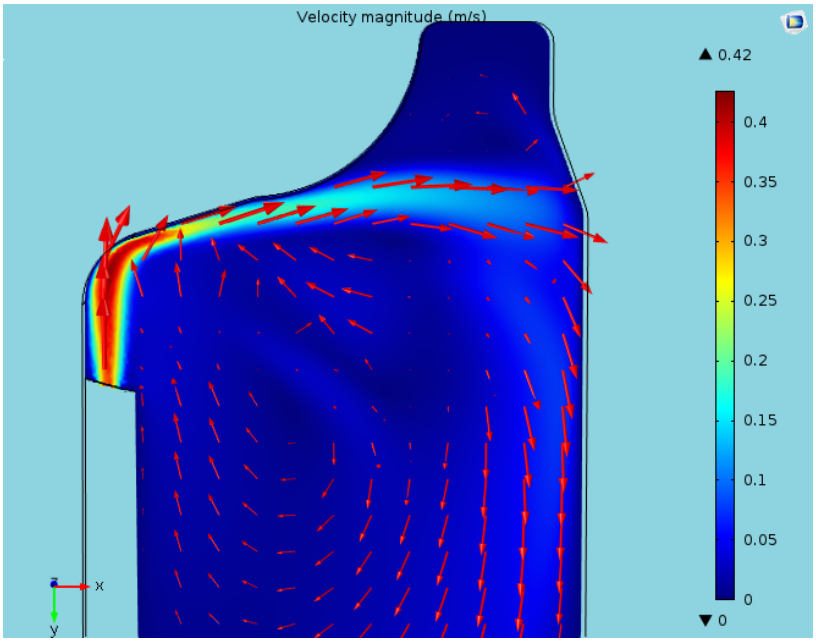

Figure 6.4: Focus on the recirculation area near the inlet surface.

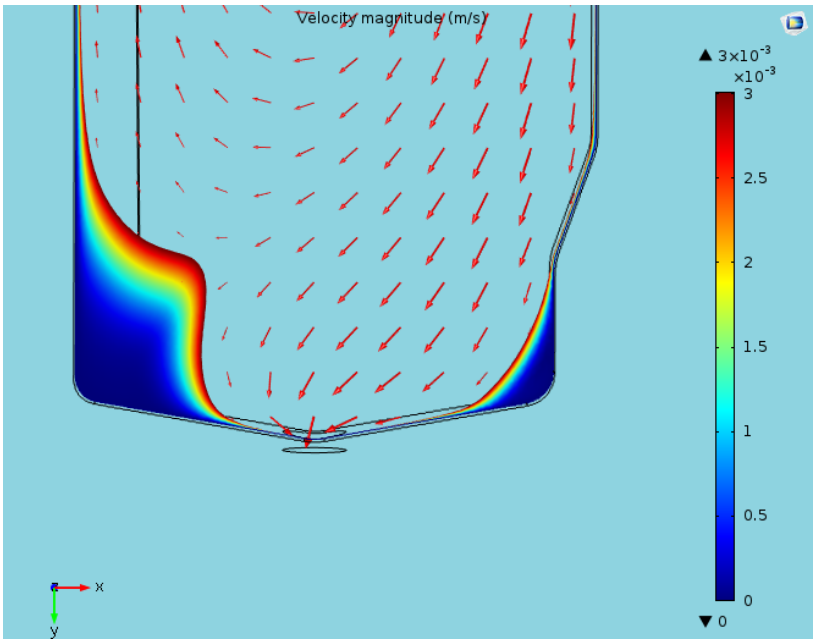

Figure 6.5: Focus on the velocity plot in the lower region of the venous chamber; the blue colour stays for 0 m/s, the red one for 0.003 m/s.

6.2 Viscous Stress

As stated in section 2.3 and 2.4, viscous shear stress higher than 8 Pa would promote platelet activation, which enhance blood coagulation. Furthermore, stresses greater than 150 Pa would produce high levels of hemolysis. Concerning these two phenomena, the drip chamber of the cassette will be considered efficient if viscous stressed inside it are lower than the threshold value for platelet activation. This way, both hemolysis and coagulation are avoided. Considering the fact that during the flow the higher shear stresses are found at the wall, Figure 6.6 represent the contour of the total wall shear stress (WSS), associating the red color to high stress and dark blue to low stress. Clearly, the highest WSS are found in the inlet region where the maximum velocity gradient are found. The wall shear stress magnitude was also measured along a surface line passing through the point where the highest stress was found and the result can be viewed in the line graph in Figure 6.8. The maximum value of the wall shear stress is 3.64 Pa, significantly below the threshold value of 8 Pa, and quite similar to typical values in normal circulation (1-3 Pa). Based on the achievements of the CFD simulation, the new design of the venous chamber is considered efficient regarding to the viscous stress.

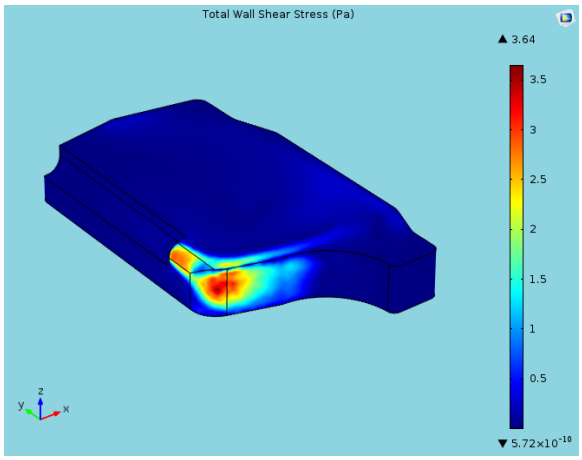

(a) Isometric view.

Figure 6.6: Contour plot of the wall shear stress.

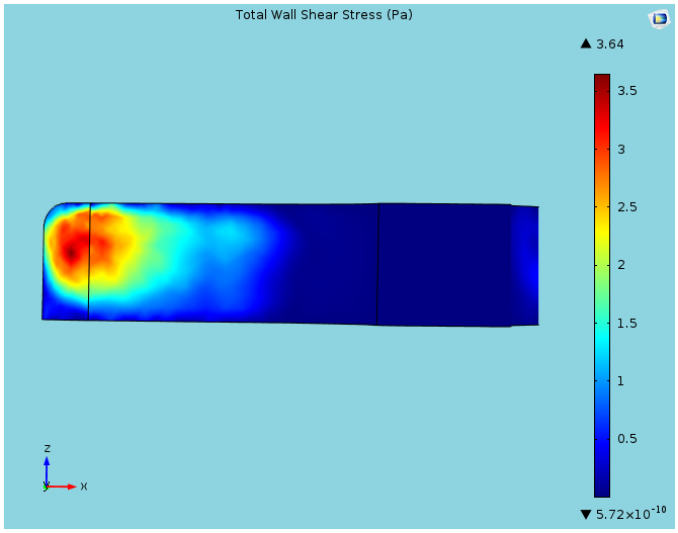

(b) Top view.

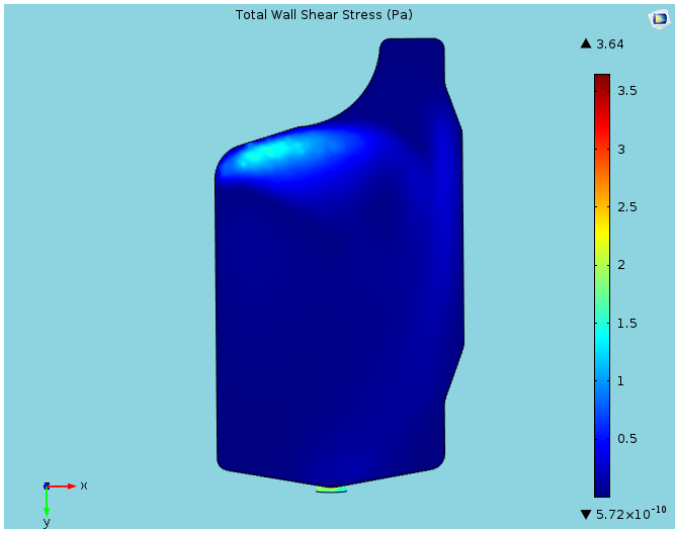

(c) Front view.

Figure 6.6: Contour plot of the wall shear stress.

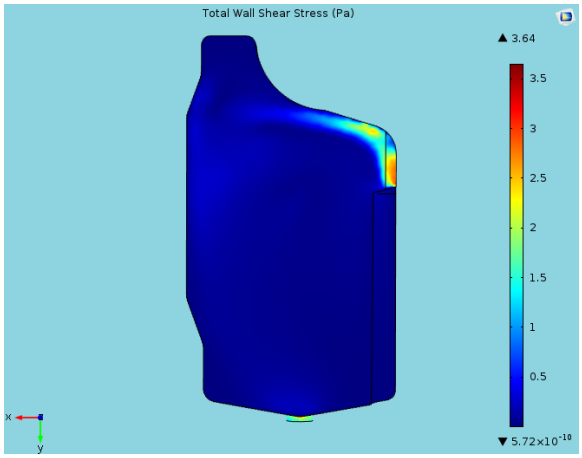

(d) Rear view.

Figure 6.6: Contour plot of the wall shear stress.

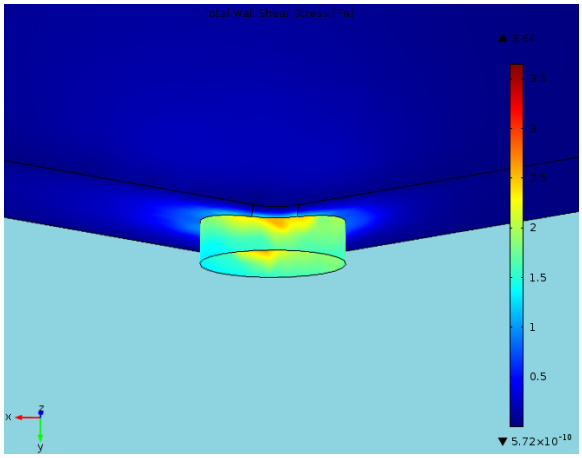

Figure 6.7: Contour plot of the wall shear stress in the outlet region.

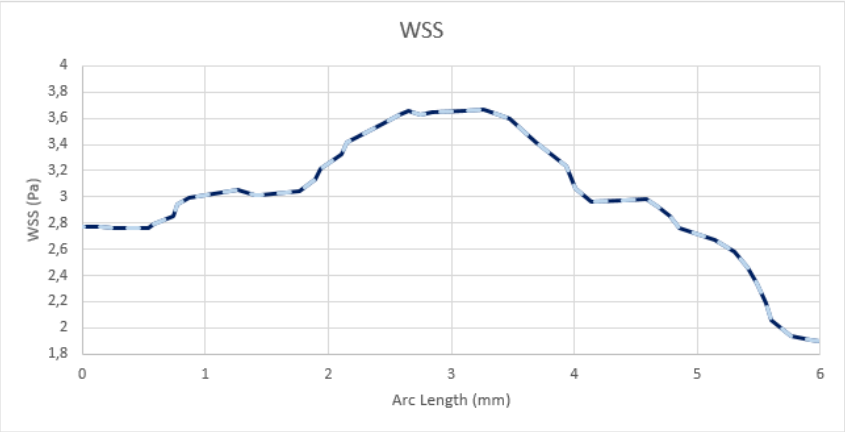

Figure 6.8: Wall shear stress magnitude as a function of arc length.

6.3 Pressure

As highlighted in section 2.3, pressure drops higher than $\Delta P = 22 \cdot 10^6$ Pa produce hemolysis due to yield stress of red cell membrane being exceeded. The knowledge of negative pressure gradients that blood encounters in its flowing through the venous chamber is of paramount importance. Figure 6.9 represents the x-y planes in which the maximum ($P_{max} = 8127$ Pa) and minimum ($P_{min} = 7998$ Pa) are found. Taking into account the preferential direction of the flow, we measured pressure and the relative gradients along two surface lines passing through the zones where the maximum gradients are found. Results can be seen in the line graphs in Figure 6.10 and Figure 6.11. The magnitude of the rate of change of pressure is evaluated based on the velocity which the red cells undergo the pressure gradient. The combined analysis of both pressure gradient and velocity magnitude yields to a maximum rate of change of pressure of 20940 Pa/s in the inlet region and of 4600 Pa/s in the outlet region. The corresponding graph are shown in Figure 6.12. Since the maximum allowable ΔP that produce no red blood cells damages is $22 \cdot 10^6$ Pa, we can affirm that the pressure field that is generated by the blood flow inside the venous chamber fulfil the requirements.

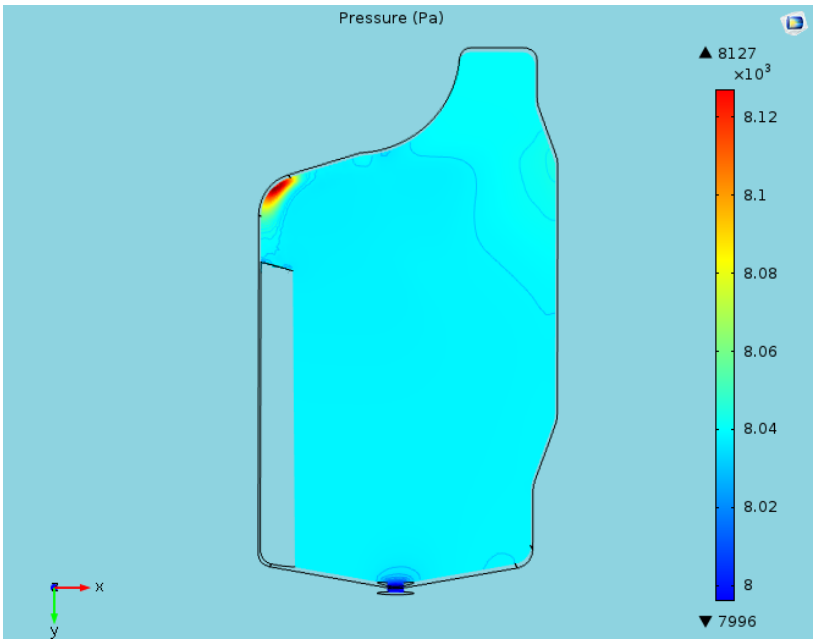

(a) Plane passes through the point of maximum pressure.

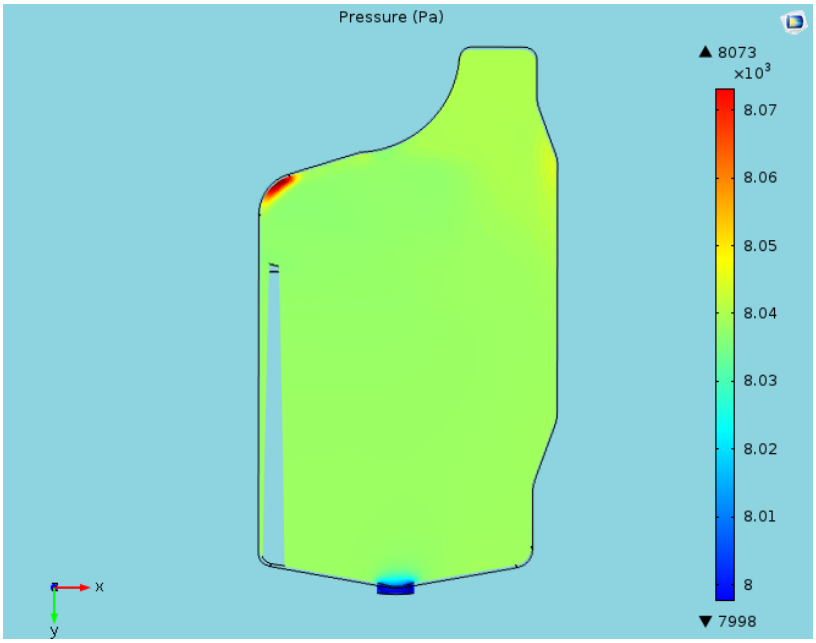

(b) Plane passes through the point of minimum pressure.

Figure 6.9: Pressure field in x-y planes.

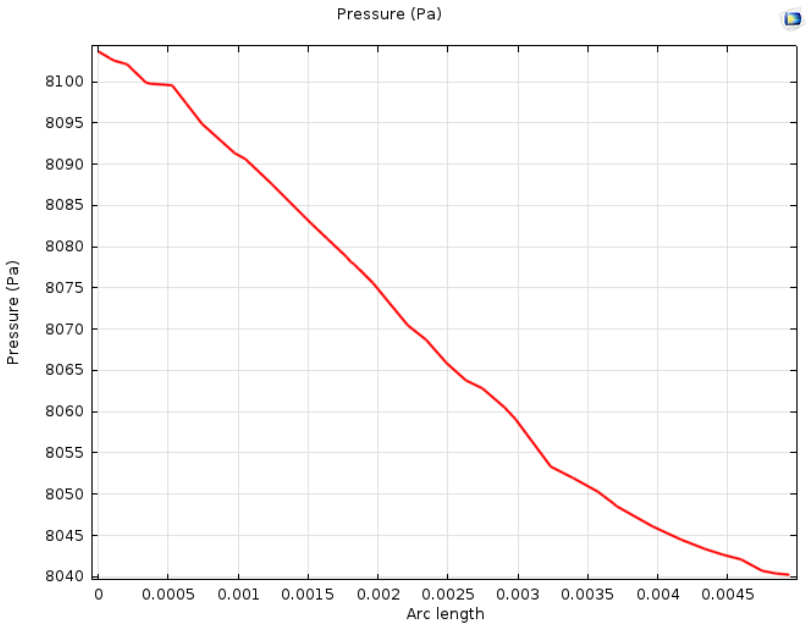

(a) Pressure magnitude.

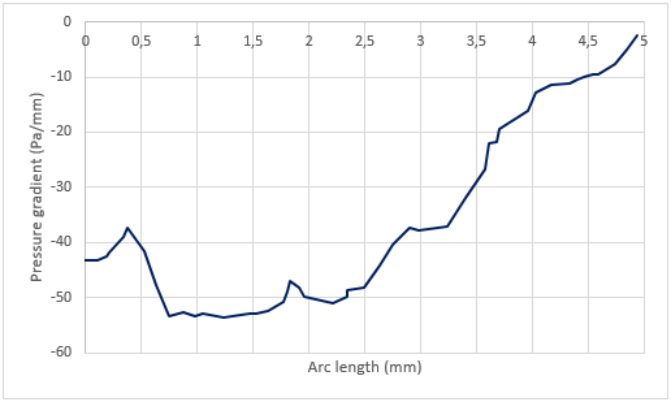

(b) Pressure gradient.

Figure 6.10: Pressure magnitude and gradient as a function of arc length in the inlet region.

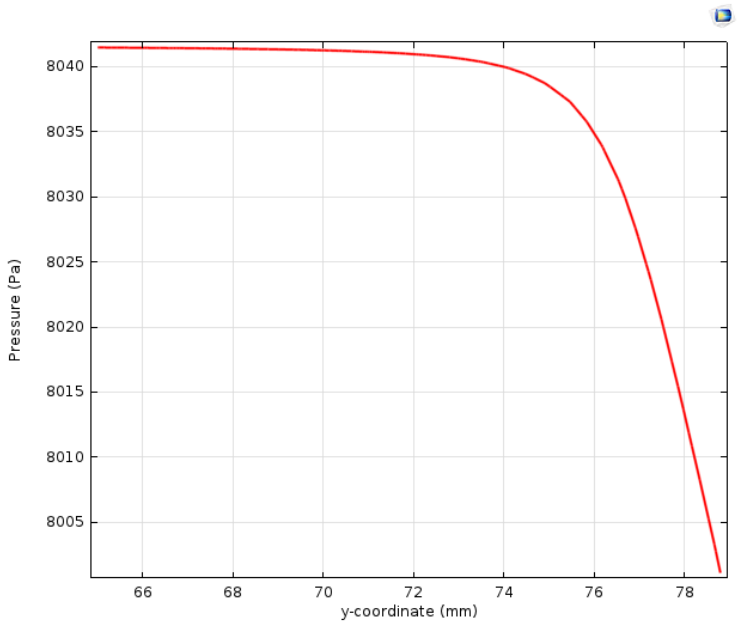

(a) Pressure magnitude.

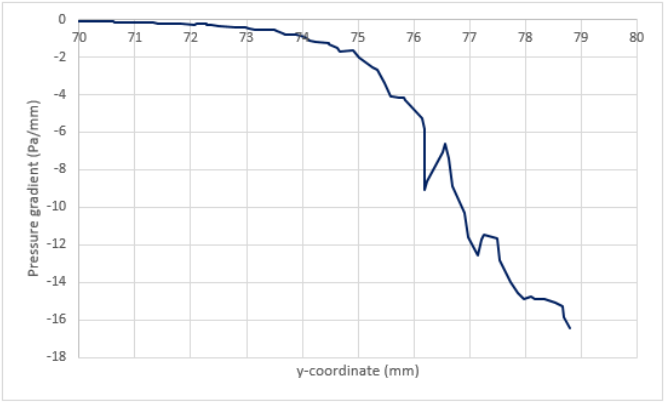

(b) Pressure gradient.

Figure 6.11: Pressure magnitude and gradient as a function of y-coordinate in the outlet region.

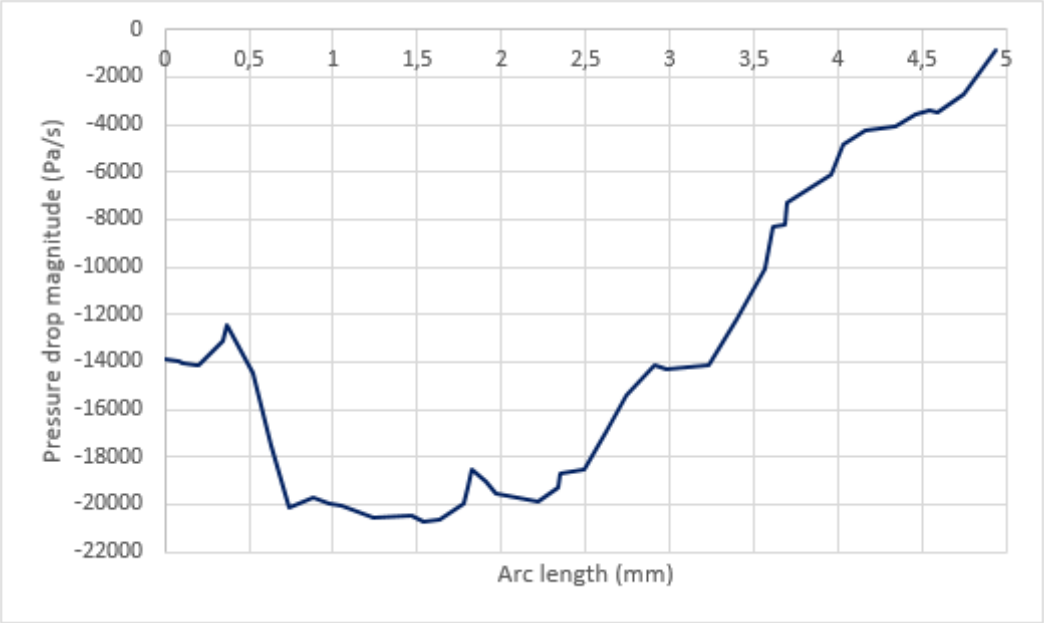

(a) Inlet region.

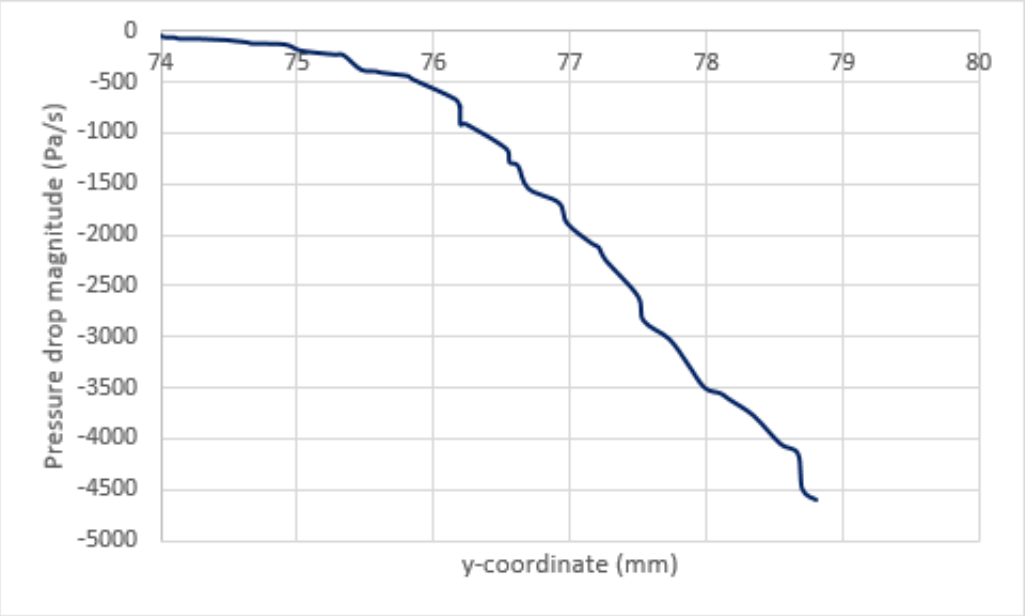

(b) Outlet region.

Figure 6.12: Pressure drop magnitude in the inlet and outlet regions.

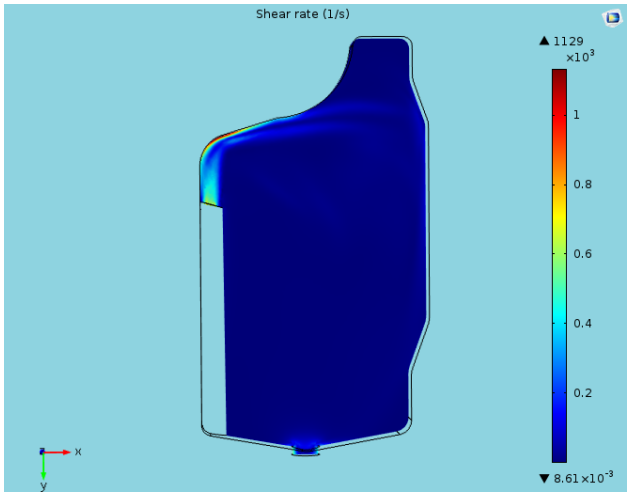

Figure 6.13: Shear rate magnitude plotted on a surface passing through the centerline of the inlet duct.

6.4 Shear Rate

Results from shear rate analysis are shown in Figure 6.13 and 6.14. Obviously the maximum shear rate is found on the upper wall of the venous chamber, near the inlet duct, on which blood impacts with a higher velocity. The maximum value of the shear rate is 1147 s^{-1}. But what matters for the purpose of this study are shear rates below the threshold value $\dot{\gamma}_t = 20s^{-1}$ that could promote coagulation. We expect to find them in the two zones at low flow speed in the bottom part of the venous chamber, which have already been highlighted in Figure 6.5. Figure 6.15 shows the shear rate on that surface plotted together with the streamlines. From the analysis of the streamlines, the presence of a preferential direction of the flow is clearly seen. Blood that is located in the two zones near the inferior edges lies outside of it and it is in a region of very low shear rate. The synergy between these two conditions suggests the possible presence of aggregation between cells that promote clotting.

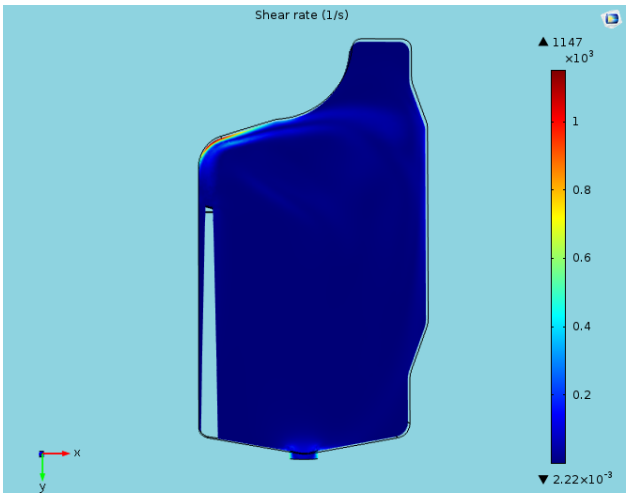

Figure 6.14: Shear rate magnitude plotted on a surface passing through the centerline of the outlet duct.

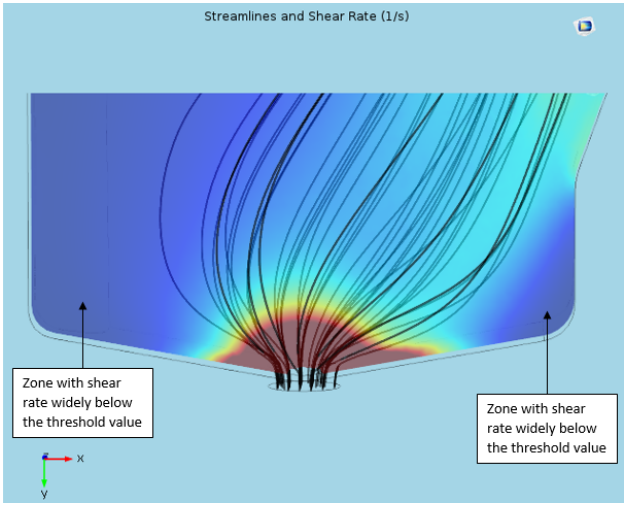

Figure 6.15: Streamlines and shear rate magnitude zoomed on a surface passing through the centerline of the outlet duct.

6.5 Conclusions and possible future works

The ultimate aim of this thesis work was the evaluation of the fluid dynamic performances of the custom drip chamber of the Bellco captive disposable device. To achieve this goal, firstly the currently used cassette and its main components were shown, their relative functions were pointed pout and materials with which the cassette is manufactured were specified. This introduction was necessary in order to show the new design of the disposable. The development of a new layout of the cassette started the last year: the fluid dynamic analysis of its venous chamber is part of this project. Subsequently, we have listed the various geometric considerations that led to the revision of the venous chamber structure and we gave reason for the choices we made regarding the selection of new materials. The productive process by which the new cassette shall be manufactured imposed all the above-mentioned modifications. The new disposable shall be co-molded: this will ensure a considerable reduction of both manufacturing times and costs and it will guarantee a higher process robustness. Ultimately, we focused on the drip chamber: a fluid dynamic simulation has been carried out, using the FEM software COMSOL Multiphysics®. The results obtained were analyzed focusing on the velocity and pressure fields and on the corresponding shear rate and shear stress generated. These are the most relevant fluid dynamic parameters for the presence or absence of phenomena such as blood hemolysis and clotting, that are the major problems that could manifest during an extracorporeal dialysis treatment. For this reason, the venous chamber is defined as fluid-dynamically efficient if the flows which develop inside it do not contribute to the occurrence of the two above-named phenomena. Results showed the presence of a well-streamlined flow combined with a recirculation zone that favors fluid mixing in the upper part of the venous chamber. In the lower region, close to the bottom edge, two areas of low velocity were highlighted. This result, analysed together the streamlines plot, suggested the possible presence of stagnation points which can promote coagulation. For that reason, we made some changes to the geometric layout of the drip chamber (bottom edges have been

rounded). The fluid dynamic efficiency of the proposed modification will be tested as soon as the supplier will provide us with the CAD model. Shear stress and pressure drop rate were calculated to be below the threshold value both for the presence of hemolysis and platelet activation that favor coagulation.

Eventually, the proposed simulation can be considered as pilot investigation. First, the numerical results must be supported by in-vitro tests, which will provide a quantitative measure of venous chamber efficiency. Secondly, to acquire a more precise understanding of the flows that develop inside the venous chamber during a dialysis treatment, a time dependent simulation should be carried out, so as to take account of the pulsatile flow originated by the peristaltic pumps. Finally, the presence of the filter on the outlet duct must be considered and its effects on the flow should be tested.

Bibliography

[1] Ahmad, S., Misra, M., Hoenich, N., Daugirdas, J., Hemodialysis Apparatus. In: Handbook of Dialysis. 4th ed. New York, 59-78, 2008.

[2] Akbari, A.,Levin, A., Hemmelgarn, B., Culleton, B., Tobe, S., McFarlane, P., Ruzicka, M., Burns, K., Manns, B., White, C., Madore, F., Tonelli, M., et al, Guidelines for the management of chronic kidney disease CMAJ 179 (11): 1154–62, 2008.

[3] Ashrafizaadeh, M., Bakhshaei, H., A comparison of non-Newtonian models for lattice Boltzmann blood flow simulations, Computers and Mathematics with Applications, p.1045-1054, 2009.

[4] Basić-Jukić, N., Kes, P., Ljutić, D., Brunetta-Gavranić, B., The role of arterial hypertension in the development of chronic renal failure, Acta Medica Croatica, 78–84, 2011.

[5] Baskurt, OK., Meiselman, HJ.,Blood Rheology and Hemodynamics, Seminars in thrombosis and hemostasis, vol.29, n.5, 2003.

[6] Bellomo, R., Moore, EM., Nichol, AD, The meaning of acute kidney injury and its relevance to intensive care and anaesthesia, Anaesthesia and intensive care 40 (6): 929–48, 2012.

[7] Blake, P., Daugirdas, J., Physiology of Peritoneal Dialysis. In: Handbook of Dialysis. 4th ed. New York, 323-338, 2008.

[8] Blausen gallery 2014, Wikiversity Journal of Medicine, DOI:10.15347/wjm/2014.010, ISSN 20018762.

[9] Boyd, J., Buick JM., Comparison of Newtonian and non-Newtonian flows in a two dimensional carotid artery model using the lattice Boltzmann method, Physics in medicine and biology, 2007.

[10] Buresti, G., Elements of Fluid Dynamics, Imperial College Press, 2012.

[11] Casciani CU., Cervelli V., De Angelis S., Splendiani G., La dialisi tecnica e clinica, 1ª ed., Roma, 2007.

[12] Casson, N., Flow equation for pigment-oil suspensions of the printing ink type, Rheology of disperse systems, ch.5, New York:Pergamon, 1959.

[13] Catapano, G., Vienken, J., Biomedical applications of membranes. Advanced membrane technology and application,489-517, 2008.

[14] Chien, S., Taylor, HM., et al., Effects of hematocrit and plasma proteins on human blood rheology at low shear rates, J.Appl.Physiol., 21(1) : 81-87, 1966.

[15] Conrad, AS., Finite Element Analysis of Fluid and Solute Transport in Hemodiafiltration Membranes, Excerpt from the Proceedings of the COMSOL User Conferences, Boston, 2005.

[16] Coresh, J., Levey, AS., K/DOQI clinical practice guidelines for chronic kidney disease, National Kidney Foundation, 2002.

[17] Davis, A., Naghavi, M., Wang, H., Lozano, R., Liang, X., Zhou, M., et al, Global, regional, and national age-sex specific all-cause and cause-specific mortality for 240 causes of death, 1990-2013: a systematic analysis for the Global Burden of Disease Study 2013, Lancet, 385, 117–171, 2015.

[18] Dorsey, R., Saydah, S., Eberhardt, M., Rios-Burrows, N., Williams D., Geiss, L., Prevalence of chronic kidney disease and associated risk factors - United States - 1999–2004, MMWR Morb. Mortal. Wkly., 56(8):161-5, 2007.

[19] Eiam-Ong, S., Tiranathanagul, K., Susantitaphong, P., Keomany, C., Mahatanan, N., Praditpornsilpa, K., Long - Term Efficacy of Pre- and Post-Dilution Online Hemodiafiltration with Dialyzer Reuse, Journal of the Medical Association of Thailand, vol. 95, 2012.

[20] Farina, JV., Gallo, G., TSC0001-01-Procedura di test membrana (durata e permeabilità) per kit bloodlines monouso (Cassette e linee sangue) per la realizzazione della dialisi con macchine Captive Bellco, Bellco internal document, 2015.

[21] Ferro, G., Pizzarelli, F., Emodiafiltrazione in pre-diluizione e in post-diluizione, Giornale Italiano Nefrologia, 29, S37-S45, 2012.

[22] Fiorenzi, A., NMB Bloodlines Specification-REV-08, Bellco internal document, 2012.

[23] Fischbach, M., Fothergill, H., Zaloszyc, A., Seuge, L., Hemodiafiltration: the addition of convective flow to hemodialysis, Pediatr Nephrol, 27:351-356,2012.

[24] Fodor, PS., Siebert, MW., Newtonian and non-Newtonian Blood Flow over a Backward-Facing Step - A Case Study, Excerpt from the proceedings of the COMSOL Conference, Boston, 2009.

[25] Gale Encyclopedia of Medicine, 2008, retrieved October 2 2015.

[26] Graaff, R., Busscher, HJ., Oeveren, VW., et al., On the influence of flow conditions and wettability on blood material interactions, in Spijker, HT., Biomaterials 24, 4717-4727, 2003.

[27] Guerra, T., Tiago, J., Improving Blood Flow Simulation Using Known Data, Excerpt from the proceeding of the COMSOL Conference, Cambridge, 2014.

[28] Harvey, B., Shaheen, I., Watson, AR., Haemofiltration therapy, Paediatrics and Child Health, vol.9121-126, 2009.

[29] Hathcock JJ., Flow effects on Coagulation and Thrombosis, Arteriosclerosis, Thrombosis, and Vascular Biology, 26(8):1729-37, 2006.

[30] Hirsch, H., Schmid-Schonbein, H., Gaehtgens, P., On the Shear Rate Dependence of Red Cell Aggregation In Vitro, The Journal of Clinical Investigation, vol.47, 1447-1454, 1968.

[31] Hung, KC., Liao, MT., Sung, CC., Wu, CC., Lo, L., Lu, KC., Insulin Resistance in Patients with Chronic Kidney Disease, Journal of Biomedicine and Biotechnology,1–5, 2012.

[32] Kallenbach, JZ., Review of Hemodialysis for nurses and dialysis personnel, 7th ed. St. Louis, Missouri, 2005.

[33] Karoor S.,Ofsthun NJ., Suzuki, M., Hemodialysis membranes. Advanced membrane technology and application, 519-539, 2008.

[34] Klag, MJ., Perneger, TV., Whelton, PK., Risk of Kidney Failure Associated with the Use of Acetaminophen, Aspirin, and Nonsteroidal Antiinflammatory Drugs, New England Journal of Medicine, 331, 1675-1679, 1994.

[35] Krishna, KY., Antaki, JF., et al., A Mathematical Model for Shear-Induced Hemolysis, Artificial Organs, 19(7):576-582, 1995.

[36] Kudela, H., Viscous flow in pipe, from http://fluid.itcmp.pwr.wroc.pl/ znmp/dydaktyka/fundam-FM/Lecture13.pdf.

[37] Kundu, PK., Cohen, IM.,Hu, HH., Ayyaswamy, PS., Fluid Mechanics, 4th ed., Academic Press, ch.17 Introduction to Biofluid Mechanics, p.765, 2008.

[38] Leverett, LB., Hellums, JD., Alfrey, CP., Lynch, EC., Red blood cell damage by shear stress, Biophysical Journal, Volume 12, 257-273, 1972.

[39] Lou, Z., Yang, WJ., A computer simulation of the non-Newtonian blood flow at the aortic bifurcation, Journal of Biomechanics, 26(1):37-49, 1993.

[40] Merril, EW., Rheology of Blood, Physiological Reviews, vol.49, n.4, 1969.

[41] Mosby's Dictionary of Medicine, Nursing and Health Professions, 7th ed., Mosby Elsevier, St. Louis, Mo., 2006.

[42] Neelamegham, S., Shankaran, H., Alexandridis, P., Aspects of hydrodynamic shear regulating shear-induced platelet activation and self-association of von Willebrand factor in suspension, bloodjournal.hematologylibrary.org, 2013.

[43] Nevaril, CG., Hellums, JD., Alfrey, CP., Lynch,EC., Physical Effects in Red Blood Cell Trauma, AIChE Journal, vol.15, n.5, p.707-711, 1968.

[44] Ogilvie, I., Silberber, C., Zieve, D., Acute kidney failure, U.S. National Library of Medicine, 2014.

[45] Rasmussen, J., Thyregod, J., Enevoldsen, MS., Henneberg, K., Using COMSOL multiphysics for Biomechanical Analysis of stent technology in cerebral aneurysms, Excerpt from the proceeding of the COMSOL Conference, Milan, 2009.

[46] Replogle, RL., Meiselman, HJ., Merril, EW., Clinical implications of blood rheology studies, Circulation, p.148-160, 1967.

[47] Ricci, Z., Ronco, C., New insights in acute kidney failure in the critically ill". Swiss Medical Weekly, 142:w13662, 2012.

[48] Sau, G., Emofiltrazione in pre- e in post-diluizione, Giornale Italiano Nefrologia, 29, S31-S36, 2012.

[49] Schowalter, WR., Mechanics of Non-Newtonian Fluids, Pergamon Press, 1978.

[50] Shen, F. Kastrup, JC., Liu, Y., Ismagilov, RF., Threshold response of initiation of blood coagulation by tissue factor in patterned microfluidic capillaries is controlled by shear rate, Arteriosclerosis, Thrombosis, and vascular biology, 2035-2041, 2005.

[51] Sochi, T., Non-Newtonian Rheology in blood circulation, 2014.

[52] Sun, J., Tijink, MSL., Wester, M., et al, A novel approach for blood purification: Mixed-matrix membranes combining diffusion and adsorption in one step, Acta Biomaterialia, 2279-2287, 2012.

[53] Sutera, SP., Flow-Induced Trauma to Blood Cells, Circulation Research, vol.41, n.1, 1977.

[54] Tank, P., Grants Dissector 15th ed., ch.4 The abdomen, p.99, 2013.

[55] Yang, WJ., Biothermal-fluid Sciences: Principles and Applications, Hemisphere Publishing Corporation, 1989.

[56] Yasuda, T., Funakubo, A., Fukui, Y., et al., Influence of Static Pressure and Shear Rate on Hemolysis of red Blood Cells, ASAIO Journal, 2001.

[57] Young, B., The Kidneys and How They Work, National Kidney and Urologic Diseases Information Clearinghouse, National Institute of Diabetes and Digestive and Kidney Diseases, 2013.

[58] Zamir, M., The Physics of Pulsatile Flow, Springer-Verlag New York, Inc., Ch 1, 2000.

[59] Web-site: http://www.alniche.com/images/alniche-img/Hemofiltration.png

[60] http://www.brookfieldengineering.com/education/viscosity-whymeasure.asp

[61] https://commons.wikimedia.org/wiki/File:Hemodialysis-en.svg/media/File:Hemodialysis-en.svg

[62] http://i25.photobucket.com/albums/c61/toXtheXendX/nephron.jpg

[63] http://www.osservatoriomalattierare.it/altre-malattie-croniche/2238-malattie-renali-croniche-ne-sono-affetti-42-mila-italiani

[64] http://www.renalresource.combookletsintropd.php

[65] http://www.slideshare.net/fergua/crrt-options-in-the-icu, slide 19 of 54

[66] http://www.treccani.it/enciclopedia/biomateriali-(Enciclopedia-della-Scienza-e-della-Tecnica)

[67] http://what-when-how.com/the-finite-element-method/computational-modelling-finite-element-method/